

# Transformers Can Implement Preconditioned Richardson Iteration for In-Context Gaussian Kernel Regression

Mingsong Yan, Dongyang Li, Charles Kulick, and Sui Tang\*

Department of Mathematics, University of California, Santa Barbara, CA

mingsongyan@ucsb.edu   dongyang\_li@ucsb.edu  
charleskulick@ucsb.edu   suitang@ucsb.edu

## Abstract

Mechanistic accounts of in-context learning (ICL) have identified iterative algorithms for linear regression and related linear prediction tasks, often using linear or ReLU attention variants. For nonlinear ICL, prior work has related softmax and kernelized attention to functional-gradient-type dynamics, but it remains unclear whether a standard transformer with softmax attention can implement a convergent solver with an end-to-end prediction-error guarantee. In this paper, we study in-context kernel ridge regression (KRR) with Gaussian kernels and show that a standard softmax-attention transformer can approximate the KRR predictor during its forward pass by implementing *preconditioned Richardson iteration* on the associated kernel linear system. Under bounded-data assumptions, we construct a *single-head* transformer with  $\mathcal{O}(\log(1/\varepsilon))$  blocks and MLP width  $\mathcal{O}(\sqrt{N}/\varepsilon)$  that achieves  $\varepsilon$ -accurate prediction for prompts of length  $N$ . Our construction reveals a functional decomposition within the transformer architecture: softmax attention produces a row-normalized Gaussian-kernel operator needed for *cross-token* interactions, while ReLU MLP layers act locally to approximate the *intra-token* scalar arithmetic required by the update. Empirically, we train GPT-2-style transformers on Gaussian-process regression tasks to further test the preconditioned Richardson interpretation. Through linear probing, we compare the transformer’s *layer-wise* predictions with the *step-wise* outputs of classical KRR solvers and find that its error profiles align most consistently with preconditioned Richardson iteration. Ablation studies further support this interpretation. Together, our theoretical construction and empirical observations identify preconditioned Richardson iteration as a concrete mechanism that softmax-attention transformers can realize for nonlinear in-context Gaussian-kernel regression.

## 1 Introduction

In-context learning (ICL) refers to the phenomenon in which a pretrained transformer, given a sequence of input-output examples followed by a query input, produces a prediction for that query in a single forward pass, *without parameter updates* [Brown et al., 2020, Garg et al., 2022]. This has emerged as a central question in the theoretical study of ICL: does the forward pass itself implement a learning algorithm on the examples in the prompt, and if so, what algorithm is being run and how is it realized by the architecture?

For linear regression and related linear tasks, prior work has made this algorithmic viewpoint precise: transformers can implement classical optimization algorithms, including gradient descent, preconditioned gradient descent, and Newton-type iterations [von Oswald et al., 2023,

---

\*Corresponding author.

Akyürek et al., 2023, Ahn et al., 2023, Bai et al., 2023, Mahankali et al., 2024, Vladymyrov et al., 2024, Fu et al., 2024, Zhang et al., 2025]. Transformer layers can be understood as steps of an iterative optimizer.

For nonlinear ICL, the corresponding mechanism is less understood. Kernel ridge regression (KRR) is a natural test scenario: nonlinear in the input but mathematically explicit, and on Gaussian process regression tasks its solution coincides with the Bayes posterior mean. Recent work analyzes attention as a form of kernel or functional gradient descent in a reproducing kernel Hilbert space (RKHS) [Cheng et al., 2024, Han et al., 2025, Dragutinović et al., 2025, Sander and Peyré, 2024]. Concrete convergence guarantees in this line, however, require attention to be *kernelized* so that each layer realizes a standard functional gradient step [Cheng et al., 2024]. Standard softmax attention corresponds instead to kernel gradient descent with a context-adaptive learning rate [Cheng et al., 2024, Sander and Peyré, 2024], for which no end-to-end convergence rate is known. Whether a standard softmax transformer implements an iterative KRR solver with end-to-end prediction-error control thus remains open.

We answer this question affirmatively for in-context KRR with Gaussian kernels. The key is to move from the primal RKHS formulation to the dual kernel linear system: given training samples  $\{(\mathbf{x}_i, y_i)\}_{i=1}^N$ , the KRR predictor admits dual coefficients  $\mathbf{w} \in \mathbb{R}^N$  that satisfy

$$(\mathbf{K} + \lambda \mathbf{I})\mathbf{w} = \mathbf{y}, \quad \mathbf{K}_{ij} = \mathcal{K}(\mathbf{x}_i, \mathbf{x}_j).$$

The mechanism question then shifts from

*“does the transformer descend a primal RKHS loss?”*

to

*“does the transformer solve the dual kernel linear system?”*

For the Gaussian kernel  $\mathcal{K}(\mathbf{x}, \mathbf{x}') = \exp(-\|\mathbf{x} - \mathbf{x}'\|^2/(2v^2))$ , suppose the raw attention score between tokens  $i$  and  $j$  is  $\mathbf{L}_{ij} = -\|\mathbf{x}_i - \mathbf{x}_j\|^2/(2v^2)$ . After softmax normalization,

$$\text{softmax}(\mathbf{L})_{ij} = \frac{\mathcal{K}(\mathbf{x}_i, \mathbf{x}_j)}{\sum_{j'=1}^N \mathcal{K}(\mathbf{x}_i, \mathbf{x}_{j'})} = (\mathbf{D}^{-1}\mathbf{K})_{ij}, \quad \mathbf{D} = \text{diag}(\mathbf{K}\mathbf{1}).$$

Softmax thus returns the kernel matrix itself with each row rescaled to sum to one, i.e., the row-sum Jacobi preconditioner of the dual kernel system. Aggregating value vectors with these weights implements the cross-token operation in a row-sum-preconditioned Richardson step; the remaining tokenwise operations (rescaling by diagonal quantities, adding the data term, updating the current iterate) are within the reach of an MLP layer. Section 4 makes this construction precise.

Figure 1 previews the empirical evidence in trained GPT-style models: the transformer’s layer-wise error trajectory closely tracks the step-wise trajectory of preconditioned Richardson iteration, while other alternatives fail to reproduce this smooth, gradual descent. Our contributions lie in making this picture concrete:

- **A dual-view mechanistic interpretation of softmax transformers** (Theorem 1; Appendix C.1). Through the dual kernel linear system, each component of a softmax-attention transformer acquires a precise algorithmic role on in-context Gaussian kernel KRR: softmax attention performs the row normalized kernel matrix-vector product, the MLP supplies the tokenwise corrections, and depth corresponds to solver iterations. This recasts nonlinear ICL with softmax from functional descent on an RKHS loss to an inexact row-sum preconditioned Richardson iteration on the dual kernel system.

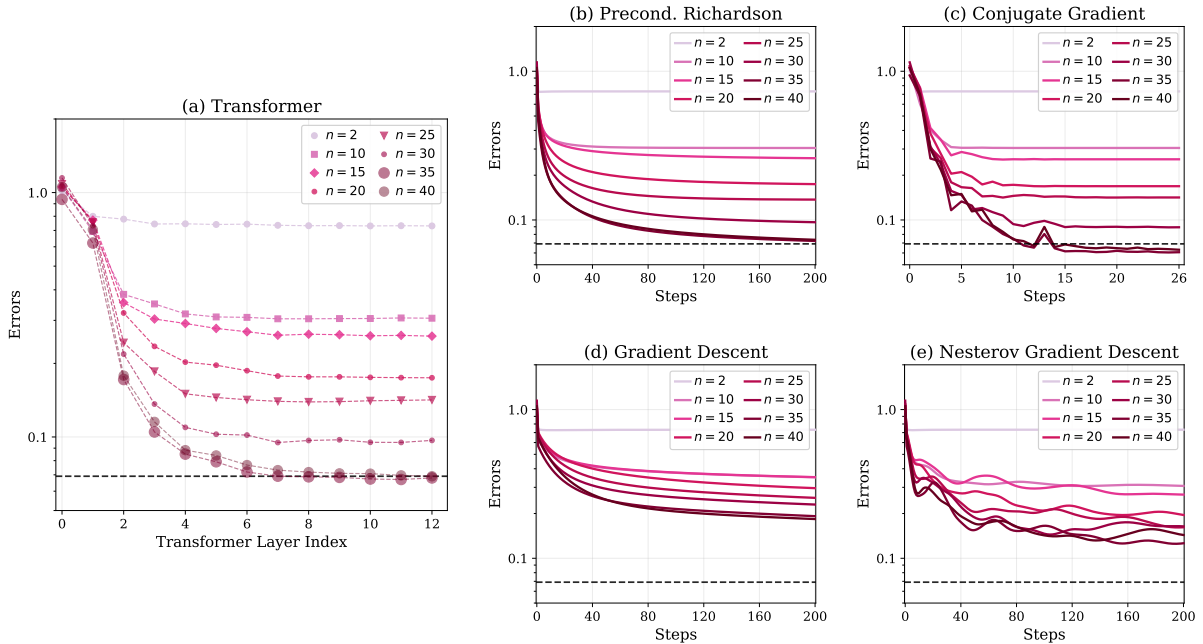


Figure 1: **Layer-wise transformer errors align with step-wise preconditioned Richardson errors.** Spherical inputs, maximum context length  $N = 40$ . All panels share the same  $y$ -axis (MSE, log scale) over context lengths  $n \in \{2, 10, 15, 20, 25, 30, 35, 40\}$ ; the dashed horizontal line in every panel marks the *transformer’s final-layer MSE at  $n = 40$*  (the empirical floor). The  $x$ -axes differ: transformer panel (a) covers layers  $\ell = 0, \dots, 12$ ; classical methods (b–e) cover their natural step budget (200 steps for Richardson/GD/Nesterov, fewer for CG). (a) Transformer MSE vs. layer index. (b) Preconditioned Richardson iteration, with a smooth, gradual descent aligning with (a) in shape. (c–e) Conjugate Gradient, which saturates within a few steps; Gradient Descent and Nesterov Gradient Descent, which descend too slowly to reach the transformer’s floor within the step budget. Full details in Section 5; replications for Uniform and Gaussian inputs in Figure 4.

- **End-to-end prediction-error guarantee with explicit depth–width scaling** (Theorem 1). Under bounded-data assumptions, a single-head softmax-attention transformer with ReLU MLP layers approximates the exact KRR predictor to prediction accuracy  $\varepsilon$  using depth  $\mathcal{O}(\log(1/\varepsilon))$  and MLP width  $\mathcal{O}(\sqrt{N}/\varepsilon)$  on prompts of length  $N$ . The depth scaling traces directly to the convergence rate of preconditioned Richardson; the width scaling, to the cost of approximating the tokenwise scalar arithmetic.
- **Empirical evidence and architectural specificity** (Section 5). We pretrain GPT-style transformers on Gaussian-process regression tasks across input distributions and prompt lengths, and use layer-wise linear probes to compare per-layer prediction errors against the per-step iterates of four classical iterative methods for KRR: preconditioned Richardson and conjugate gradient applied to the kernel linear system, and gradient descent and Nesterov gradient descent applied to the RKHS-regularized loss. Preconditioned Richardson is the unique method whose per-step error trajectory aligns with the transformer’s per-layer error trajectory across all settings tested; both produce a smooth, gradual descent with the same fan structure across context lengths. Ablations confirm this alignment is structurally specific: changing the Gaussian kernel or replacing softmax with linear attention weakens it, and

a noise-mismatch ablation supports interpreting the trained transformer as a finite-iterate preconditioned Richardson solver with a fixed regularizer baked into the weights.

## 2 Related work

**Algorithmic interpretations of ICL.** A major line of research frames the transformer’s forward pass as the execution of a learning algorithm on the prompt. Garg et al. [2022] empirically showed that transformers can be trained to solve linear regression and decision-tree tasks in context. Subsequent theoretical work has focused predominantly on *linear regression*, identifying gradient descent [von Oswald et al., 2023, Akyürek et al., 2023], preconditioned gradient descent [Ahn et al., 2023, Mahankali et al., 2024, Vladymyrov et al., 2024], and Newton-type iterations [Fu et al., 2024], with parallel analyses of training dynamics [Zhang et al., 2024a, Chen et al., 2024, Lu et al., 2025, Zhang et al., 2025, Huang et al., 2024]. Beyond linear regression, this line covers algorithm selection across linear tasks [Bai et al., 2023], nearest-neighbor classification [Li et al., 2024], discrete and Boolean function learning [Bhattamishra et al., 2024], and formal-language learning [Akyürek et al., 2024]. A growing subline examines the role of MLPs: Zhang et al. [2024b] show that adding an MLP block to linear attention enables one-step gradient descent with learnable initialization for linear regression; Sun et al. [2025] prove that linear self-attention (LSA) alone cannot outperform linear predictors on nonlinear tasks and construct LSA+MLP architectures for nonlinear function classes; Demir and Dogan [2025] establish an asymptotic equivalence between random Transformers with nonlinear MLP heads and finite-degree polynomial predictors. Most of these constructions abstract away standard transformer nonlinearities: attention is taken to be linear or non-softmax, MLPs are restricted to polynomial or random-feature regimes, or both. Our work operates in the standard softmax-attention / ReLU-MLP setting and identifies preconditioned Richardson iteration on the dual kernel system as a concrete mechanism for nonlinear in-context regression, assigning precise algorithmic roles to both components: softmax attention performs the preconditioned cross-token kernel matrix vector product, and MLPs supply the tokenwise scalar arithmetic that completes each Richardson step.

**Kernel and softmax views of nonlinear ICL.** A complementary line connects ICL to kernel-based prediction. Cheng et al. [2024] show that attention with a kernel-matched activation implements functional gradient descent in the corresponding RKHS for nonlinear regression, whereas standard softmax attention does not directly define a kernel function because of its context-dependent normalization. Han et al. [2025] show that Bayesian inference on in-context prompts is asymptotically equivalent to normalized kernel regression, Collins et al. [2024] connect softmax attention to Nadaraya–Watson kernel estimation and nearest-neighbor prediction, and Shen et al. [2025] study a kernel-regression view on manifold-structured data with intrinsic-dimension generalization bounds; these are statistical or estimator-level characterizations rather than finite-depth algorithmic constructions. Dragutinović et al. [2025] demonstrate that a single softmax-attention layer realizes one context-adaptive step of kernel gradient descent for cross-entropy classification; this is a single-layer characterization on a classification objective and does not provide an end-to-end multi-layer convergence rate. To our knowledge, no prior work delivers, for standard softmax-attention transformers on a nonlinear in-context regression task, an end-to-end prediction-error guarantee whose depth scaling is controlled by the convergence rate of the underlying solver. The dual-system viewpoint developed here is what enables this: by working in the finite-dimensional kernel system rather than in an RKHS, we pinpoint the iteration as inexact preconditioned Richardson, give explicit depth–width estimates, and assign each architectural component a precise algorithmic role.

### 3 Preliminaries

#### 3.1 Transformers

We consider transformer architectures that operate on an input sequence of  $N$  tokens, represented by a feature matrix  $\mathbf{Z} = [\mathbf{z}_1, \dots, \mathbf{z}_N] \in \mathbb{R}^{D \times N}$  whose  $i$ -th column  $\mathbf{z}_i \in \mathbb{R}^D$  is the embedding of the  $i$ -th token. We consider the following transformer architecture [Vaswani et al., 2017].

**Definition 1** (Softmax attention layer). A multi-head attention layer with  $H$  heads is denoted by  $\text{Attn}(\cdot)$ . For each head  $h \in [H]$ , let  $\mathbf{W}_Q^{(h)}, \mathbf{W}_K^{(h)}, \mathbf{W}_V^{(h)} \in \mathbb{R}^{D \times D}$  be the query, key, and value matrices, and let  $\mathbf{M}^{(h)} \in \{0, -\infty\}^{N \times N}$  be a mask matrix. Given  $\mathbf{Z} \in \mathbb{R}^{D \times N}$ , the layer outputs  $\tilde{\mathbf{Z}} = \text{Attn}(\mathbf{Z})$  via the residual update

$$\tilde{\mathbf{Z}} := \mathbf{Z} + \sum_{h=1}^H (\mathbf{W}_V^{(h)} \mathbf{Z}) \cdot \sigma((\mathbf{W}_K^{(h)} \mathbf{Z})^\top (\mathbf{W}_Q^{(h)} \mathbf{Z}) + \mathbf{M}^{(h)}),$$

where  $\sigma(\cdot)$  is the row-wise softmax. Equivalently, for each  $i \in [N]$ ,

$$\tilde{z}_i = z_i + \sum_{h=1}^H \sum_{j=1}^N \frac{\exp(\langle \mathbf{W}_Q^{(h)} z_i, \mathbf{W}_K^{(h)} z_j \rangle + M_{ij}^{(h)})}{\sum_{j'=1}^N \exp(\langle \mathbf{W}_Q^{(h)} z_i, \mathbf{W}_K^{(h)} z_{j'} \rangle + M_{ij'}^{(h)})} \mathbf{W}_V^{(h)} z_j.$$

**Definition 2** (MLP layer). An MLP layer with hidden dimension  $D'$ , denoted  $\text{MLP}(\cdot)$ , has weight matrices  $\mathbf{W}_{\text{in}}, \mathbf{W}_{\text{out}} \in \mathbb{R}^{D \times D'}$  and acts pointwise on each token: for  $\mathbf{Z} \in \mathbb{R}^{D \times N}$ ,  $\text{MLP}(\mathbf{Z}) := \mathbf{Z} + \mathbf{W}_{\text{out}} \sigma(\mathbf{W}_{\text{in}} \mathbf{Z})$ , where  $\sigma(t) = \max\{t, 0\}$  is the entrywise ReLU activation.

**Definition 3** (Transformer block and  $L$ -block transformer). A transformer block (TFB) is the composition  $\text{TFB}(\mathbf{Z}) := \text{MLP}(\text{Attn}(\mathbf{Z}))$  of an attention layer followed by an MLP layer; we also allow an MLP-only block  $\text{TFB}_0$  in which the attention layer acts as the identity (e.g., by setting all value matrices to zero), so  $\text{TFB}_0(\mathbf{Z}) = \text{MLP}(\mathbf{Z})$ . An  $L$ -block transformer TF is the sequential composition  $\text{TF}(\mathbf{Z}) := (\text{TFB}^{(L)} \circ \text{TFB}^{(L-1)} \circ \dots \circ \text{TFB}^{(1)})(\mathbf{Z})$  of  $L$  blocks.

#### 3.2 In-context Learning for Kernel Ridge Regression

**Kernel ridge regression.** Let  $\mathcal{D} = \{(\mathbf{x}_i, y_i)\}_{i=1}^N$  be a given training dataset. Here,  $\{\mathbf{x}_i\}_{i=1}^N \subset \mathbb{R}^d$  represent the input vectors,  $\{y_i\}_{i=1}^N \subset \mathbb{R}$  are the corresponding labels. We formulate the classical kernel ridge regression problem within a Reproducing Kernel Hilbert Space (RKHS)  $\mathcal{H}$  associated with a reproducing kernel  $\mathcal{K}$ . The objective is to minimize the regularized empirical risk

$$\min_{f \in \mathcal{H}} \left\{ \frac{1}{N} \sum_{i=1}^N (f(\mathbf{x}_i) - y_i)^2 + \lambda_0 \|f\|_{\mathcal{H}}^2 \right\}, \quad (1)$$

where  $\lambda_0 > 0$  is the regularization parameter. By the Representer Theorem [Schölkopf et al., 2001], the optimal solution admits the finite-dimensional form  $f^*(\cdot) = \sum_{i=1}^N w_i \mathcal{K}(\mathbf{x}_i, \cdot)$ . In the RKHS setting considered here, optimizing over the dual coefficients  $\mathbf{w} = [w_1, \dots, w_N]^\top \in \mathbb{R}^N$  yields the explicit dual linear system

$$(\mathbf{K} + \lambda \mathbf{I}) \mathbf{w} = \mathbf{y}, \quad (2)$$

with kernel matrix  $\mathbf{K}_{ij} = \mathcal{K}(\mathbf{x}_i, \mathbf{x}_j)$ , label vector  $\mathbf{y} = [y_1, \dots, y_N]^\top$ , and  $\lambda := \lambda_0 N$ .

This formulation has a clean statistical interpretation [Rasmussen and Williams, 2006, Caponnetto and De Vito, 2007]. Suppose the training labels are generated as  $y_i = f(\mathbf{x}_i) + \epsilon_i$ , where  $f$

is drawn from a zero-mean Gaussian process with covariance kernel  $\mathcal{K}$ , denoted  $f \sim \text{GP}(0, \mathcal{K})$ , and  $\epsilon_i \sim \mathcal{N}(0, \sigma^2)$  are i.i.d. observation noises. If the test label is the noiseless latent value  $y_{N+1} = f(\mathbf{x}_{N+1})$ , then setting  $\lambda = \sigma^2$  makes the KRR predictor  $f^*(\mathbf{x}_{N+1})$  coincide with the Bayes posterior mean.

**Iterative solution via preconditioned Richardson iteration.** As discussed in the introduction, the row-sum diagonal  $\mathbf{D} = \text{diag}(\mathbf{K}\mathbf{1})$  acts as a preconditioner: left-multiplying (2) by  $\mathbf{D}^{-1}$  gives the equivalent system  $\mathbf{D}^{-1}(\mathbf{K} + \lambda\mathbf{I})\mathbf{w} = \mathbf{D}^{-1}\mathbf{y}$ , on which the preconditioned Richardson iteration with step size  $\eta > 0$  reads

$$\mathbf{w}^{(\ell+1)} = \mathbf{w}^{(\ell)} + \eta (\mathbf{D}^{-1}\mathbf{y} - \mathbf{D}^{-1}(\mathbf{K} + \lambda\mathbf{I})\mathbf{w}^{(\ell)}). \quad (3)$$

Iteration (3) is the update that the transformer construction in Section 4 approximately implements step by step in its forward pass.

**In-context learning.** For in-context learning, the transformer receives the training dataset  $\mathcal{D}$ , a new test input  $\mathbf{x}_{N+1} \in \mathbb{R}^d$ , and a set of auxiliary weights  $\{w_i\}_{i=1}^N$  that act as placeholders for the intermediate iterates  $\mathbf{w}^{(\ell)}$  in (3); the construction in Section 4 updates these weights through depth and reads off the prediction at  $\mathbf{x}_{N+1}$ .

To facilitate the required mathematical operations within the transformer’s forward pass, we adopt two simple input augmentations: we include the squared norms  $\|\mathbf{x}_j\|^2$  as a feature of each token (or, in the unit-norm setting, this feature is constant and can be omitted [Dragutinović et al., 2025]), and we prepend the sequence with a designated dummy token  $\mathbf{x}_0 = \mathbf{0}$ . We view these augmentations as *input preprocessing* rather than part of the core iterative-solver mechanism. This is consistent with prior constructive analyses of ICL, where input encoding, initialization, or readout operations are often separated from the main algorithmic update [von Oswald et al., 2023, Bai et al., 2023, Fu et al., 2024]. Indeed, the squared-norm feature  $\|\mathbf{x}_j\|^2$  can be approximated by an MLP-only transformer block; the dummy token  $\mathbf{x}_0 = \mathbf{0}$  is also a mild input convention, analogous to special sequence tokens such as beginning-of-sequence markers in autoregressive language models [Touvron et al., 2023]. We hard-code both in the input embedding to keep the iterative-solver mechanism clean.

Formally, we construct the input matrix  $\mathbf{Z} \in \mathbb{R}^{D \times (N+2)}$  as follows. The sequence consists of  $N + 2$  tokens indexed by  $j \in \{0, 1, \dots, N, N + 1\}$ . For each token  $j$ , we concatenate the input vector  $\mathbf{x}_j \in \mathbb{R}^d$ , the label  $y_j \in \mathbb{R}$ , the weight  $w_j \in \mathbb{R}$ , and the augmented feature  $\|\mathbf{x}_j\|^2$ . We reserve 5 dimensions padded with zeros for intermediate computation (cached memory). Finally, we append structural indicators  $\{s_j, t_j\}$  and a constant bias term. This yields the following block matrix representation for the input data

$$\mathbf{Z} = \begin{bmatrix} \mathbf{x}_0 & \mathbf{x}_1 & \mathbf{x}_2 & \dots & \mathbf{x}_N & \mathbf{x}_{N+1} \\ 0 & y_1 & y_2 & \dots & y_N & 0 \\ 0 & w_1 & w_2 & \dots & w_N & 0 \\ 0 & \|\mathbf{x}_1\|^2 & \|\mathbf{x}_2\|^2 & \dots & \|\mathbf{x}_N\|^2 & \|\mathbf{x}_{N+1}\|^2 \\ \mathbf{0}_5 & \mathbf{0}_5 & \mathbf{0}_5 & \dots & \mathbf{0}_5 & \mathbf{0}_5 \\ s_0 & s_1 & s_2 & \dots & s_N & s_{N+1} \\ t_0 & t_1 & t_2 & \dots & t_N & t_{N+1} \\ 1 & 1 & 1 & \dots & 1 & 1 \end{bmatrix} \in \mathbb{R}^{D \times (N+2)},$$

where  $D = d + 11$ , and  $\mathbf{0}_5 \in \mathbb{R}^5$  denotes a zero vector. The structural indicators act as positional encodings for the model to identify the dummy and test tokens. Specifically, the dummy token indicator  $s_j$  is defined by  $s_0 = 1$  and  $s_j = 0$  for all  $j \in [N + 1]$ ; the test token

indicator  $t_j$  is defined by  $t_{N+1} = 1$  and  $t_j = 0$  for all  $j \in \{0, 1, \dots, N\}$ . Applying the transformer to the input matrix  $\mathbf{Z}$  yields the output  $\tilde{\mathbf{Z}} = \text{TF}(\mathbf{Z})$ , from which we extract the prediction for the test token via a readout function  $y_{N+1} = \text{readout}(\tilde{\mathbf{Z}}) := \tilde{\mathbf{Z}}_{d+1, N+1}$ .

## 4 Main Result: An End-to-End Construction

We construct a single-head softmax-attention transformer with ReLU MLPs whose forward pass approximately implements preconditioned Richardson iteration (3) for the kernel system (2), with explicit bounds on the required depth and MLP width.

**Assumptions.** We impose a *bounded data* assumption: there exist  $B_x, B_y > 0$  such that  $\|\mathbf{x}_i\|_2 \leq B_x$  and  $|y_i| \leq B_y$  for all  $i \in [N + 1]$ . The kernel is the Gaussian kernel  $\mathcal{K}(\mathbf{x}, \mathbf{x}') = \exp(-\|\mathbf{x} - \mathbf{x}'\|_2^2 / (2v^2))$  with bandwidth  $v$ , and the dual coefficients are initialized to zero,  $\mathbf{w}^{(0)} = \mathbf{0}$ .

**Theorem 1 (Informal).** Fix  $c \in (0, 1)$  and  $\varepsilon \in (0, c)$ , and let  $\mathbf{w}^* = [w_i^* : i \in [N]]$  denote the solution to the KRR linear system (2). There exists a single-head transformer TF with  $2L + 5$  blocks (three read-in blocks, two blocks for each of the  $L$  iteration steps, and two read-out blocks) for  $L = \mathcal{O}(\log(1/\varepsilon))$  and MLP width  $\mathcal{O}(\sqrt{N}/\varepsilon)$  such that

$$\left| \text{readout}(\text{TF}(\mathbf{Z})) - \sum_{i=1}^N w_i^* \mathcal{K}(\mathbf{x}_i, \mathbf{x}_{N+1}) \right| \leq C_{\text{sys}} \varepsilon.$$

The system constant  $C_{\text{sys}}$  depends on regularization parameter  $\lambda_0$ , kernel bandwidth  $v$ , step size  $\eta$ , data bounds  $B_x, B_y$ , and constant  $c$ , but is independent of the prompt length  $N$ .

The formal version of the above theorem appears as Theorem 12 in Appendix C.5, with explicit estimates for the depth, MLP width, and the  $N$ -independent constant  $C_{\text{sys}}$ . The proof is constructive, and we sketch the network construction here; a full overview is given in Appendix C.1. The transformer is built in three phases. The *read-in phase* (Appendix C.2) uses three blocks to prepare quantities needed by the iterative solver, including approximations of  $\mathbf{D}^{-1}$  and  $\mathbf{D}^{-1}\mathbf{y}$ . The *iteration phase* (Appendix C.3) uses pairs of transformer blocks to approximately implement preconditioned Richardson updates for the coefficients  $\mathbf{w}$ . Finally, the *read-out phase* (Appendix C.4) extracts the prediction at the test token  $\mathbf{x}_{N+1}$ , yielding an approximation of  $\sum_{i=1}^N w_i^* \mathcal{K}(\mathbf{x}_i, \mathbf{x}_{N+1})$ .

**Algorithm-Architecture correspondence.** Across these phases, the two components of a standard transformer play complementary algorithmic roles. Softmax attention handles the *cross-token* operations: it produces row-normalized kernel interactions and computes products such as  $\mathbf{D}^{-1}\mathbf{K}\mathbf{w}^{(\ell)}$ . ReLU MLPs act locally at each token, approximating the *intra-token* scalar arithmetic, including elementwise operations such as  $\mathbf{D}^{-1}\mathbf{y}$  and  $\mathbf{D}^{-1}\mathbf{w}^{(\ell)}$ . This separation of roles is central to our transformer construction: its forward pass implements an inexact preconditioned Richardson iteration within the standard softmax-attention/MLP architecture.

**Scaling of depth and width.** The depth and width scalings in Theorem 1 come from two different sources. The depth  $\mathcal{O}(\log(1/\varepsilon))$  is an *algorithmic count* obtained from the error analysis of the inexact preconditioned Richardson iteration (Appendix A). With a suitable choice of step size  $\eta$ , the error-propagation matrix of the underlying iteration is contractive. Consequently, a logarithmic number of inexact iteration steps suffices to reach the desired prediction

accuracy. In contrast, the MLP width scaling is an *approximation count*: ReLU MLPs are used to approximate the tokenwise scalar arithmetic operations required by the construction (Appendix B). Common single-layer ReLU approximation results used in the ICL literature are input-dimension-free, thereby avoiding the curse of dimensionality [Bach, 2017, Bai et al., 2023]. In our construction, however, the MLPs only need to approximate a few specific one-dimensional smooth functions, such as  $x/(1-x)$ ,  $x^2$ , and  $1/x$ , on intervals of interest. We can therefore use explicit linear spline approximations, which are representable by single-layer ReLU networks and achieve sharper interpolation rates [De Boor, 1978, DeVore, 1998, DeVore et al., 2021]. By carefully estimating the relevant approximation intervals and error tolerances, we obtain the required MLP width scaling  $\mathcal{O}(\sqrt{N/\varepsilon})$  for each scalar approximation. Together, the depth scaling reflects the convergence rate of the inexact preconditioned Richardson iteration, while the width scaling reflects the cost of approximating the local scalar arithmetic.

## 5 Experiments

We empirically test the algorithmic identification through four claims: (i) preconditioned Richardson is the unique classical method whose per-step dynamics align with the transformer’s per-layer dynamics (Section 5.1); (ii) this alignment relies on two structural ingredients, softmax row-normalization and the Gaussian kernel (Section 5.2); (iii) it is robust across natural architectural variations (Section 5.3); and (iv) the trained transformer behaves as if regularizing with a fixed  $\lambda \approx \sigma_{\text{train}}^2$  and exhibits implicit early stopping under noise mismatch (Section 5.4).

**Data generation.** We consider dynamically generated Gaussian process (GP) regression tasks. Both training and evaluation sequences are constructed as follows. The inputs  $\mathbf{x}_i$ ,  $i \in [N+1]$ , are independent and identically distributed (i.i.d.) samples drawn from a prescribed distribution  $\mathcal{P}$ . Then, a latent function  $f \sim \text{GP}(0, \mathcal{K})$  is sampled, where  $\mathcal{K}$  is a Gaussian kernel with bandwidth  $v$ . The context labels are generated with observation noise as  $y_i = f(\mathbf{x}_i) + \epsilon_i$ , where  $\epsilon_i \sim \mathcal{N}(0, \sigma_{\text{noise}}^2)$  for  $i \in [N]$ . Unless otherwise stated, we use a maximum prompt length  $N = 40$ , input dimension  $d = 5$ , noise standard deviation  $\sigma_{\text{noise}} = 0.05$ , and kernel bandwidth  $v = 1$ . We consider three input distributions  $\mathcal{P}$ : Uniform  $\text{Unif}([-1, 1]^d)$ , Gaussian  $\mathcal{N}(0, 0.6^2 \mathbf{I}_d)$ , and Spherical  $\text{Unif}(\mathbb{S}^{d-1})$ .

**Transformer architecture and pretraining.** We pretrain a GPT-2 style decoder-only transformer [Radford et al., 2019, Garg et al., 2022] from scratch on each input distribution. The model receives the interleaved sequence  $(\mathbf{x}_1, y_1, \dots, \mathbf{x}_N, y_N, \mathbf{x}_{N+1}, 0)$  and is trained to minimize the mean-squared error between its prediction and the noisy label at every in-context position  $n \in \{1, \dots, N\}$ , following the standard ICL-regression objective [Garg et al., 2022], so the model learns to predict at every context length rather than only at  $n = N$ . By default, we use a 12-layer transformer with 8 softmax attention heads, embedding dimension 256, GELU MLPs, and Pre-LayerNorm; this deliberately differs from the construction’s single-head, ReLU-MLP, no-LayerNorm setup, so that the experiments test whether the Richardson signature is visible in a standard GPT-style variant rather than only in the hand-constructed architecture. Pretraining runs for 500,000 optimizer steps with batch size 64 (approximately 32M fresh GP sequences sampled on the fly), using AdamW with a cosine learning-rate schedule. Evaluation uses 256 freshly-sampled GP sequences with a fixed random seed shared across the transformer and all classical baselines, so per-sequence comparisons are deterministic. Full hyperparameters are in Appendix E.

**Classical baselines.** We compare the per-layer transformer predictions against four classical iterative methods for KRR. Two are linear-system solvers applied to the kernel system (2): *pre-*

conditioned Richardson iteration and conjugate gradient (CG). The other two are loss-function optimizers applied to the RKHS-regularized loss  $L(\mathbf{w}) = \frac{1}{2}\|\mathbf{K}\mathbf{w} - \mathbf{y}\|^2 + \frac{1}{2}\lambda\mathbf{w}^\top\mathbf{K}\mathbf{w}$ : gradient descent (GD) and Nesterov gradient descent. Full details for each method are provided in Appendix D.

## 5.1 Preconditioned Richardson uniquely aligns with per-layer dynamics

**Error curves.** Figure 1 compares the layer-wise MSE of the transformer with the four classical methods. *Preconditioned Richardson iteration shows the closest agreement with the transformer’s performance.* Both exhibit a smooth decrease in error and maintain similar relative spacing between the curves for different context lengths  $n$ . In contrast, the other methods show distinct behaviors: CG converges faster and follows an oscillatory error curve, while the loss-function optimizers GD and Nesterov GD are significantly slower and do not reach the transformer’s error floor. Despite prior ICL theory predominantly modeling transformers as gradient-based loss optimizers [von Oswald et al., 2023, Akyürek et al., 2023, Ahn et al., 2023, Mahankali et al., 2024], our results suggest that for KRR, the transformer is better characterized as an iterative linear-system solver.

**Similarity of errors.** To quantify the alignment between the learned transformer and classical iterative algorithms, we adapt the similarity of errors metric proposed by Fu et al. [2024]. Let  $B = \{\mathbf{x}_i, y_i\}_{i=1}^{N+1}$  be a data sequence sampled from a batch  $\mathcal{B}$  of test sequences. For a classical algorithm  $\mathcal{A}$  evaluated at iteration  $t$ , let  $\mathcal{A}^{(t)}(\mathbf{x}_{n+1} \mid \{\mathbf{x}_i, y_i\}_{i=1}^n)$  denote its prediction on the  $(n+1)$ -th example after observing a context of length  $n$ . For brevity, we write  $\mathcal{A}^{(t)}(\mathbf{x}_{n+1})$ . The vector of prediction errors across the entire sequence is defined by  $\mathbf{e}(\mathcal{A}^{(t)}|B) := [\mathcal{A}^{(t)}(\mathbf{x}_2) - y_2, \dots, \mathcal{A}^{(t)}(\mathbf{x}_{N+1}) - y_{N+1}]^\top$ . Similarly, for the transformer (TF), let  $\text{TF}^{(\ell)}(\mathbf{x}_{n+1})$  denote the scalar prediction mapped by a linear probe from the hidden state at position  $n$  in layer  $\ell$ . Its corresponding error vector on the sequence is denoted as  $\mathbf{e}(\text{TF}^{(\ell)}|B)$ . The similarity of errors (SimE) between the transformer at layer  $\ell$  and the classical algorithm at step  $t$  is defined as the expected cosine similarity of their error vectors over the test sequences  $\text{SimE}(\ell, t) := \frac{1}{|\mathcal{B}|} \sum_{B \in \mathcal{B}} \mathcal{C}(\mathbf{e}(\text{TF}^{(\ell)}|B), \mathbf{e}(\mathcal{A}^{(t)}|B))$ , where  $\mathcal{C}(\mathbf{u}, \mathbf{v}) := \frac{\langle \mathbf{u}, \mathbf{v} \rangle}{\|\mathbf{u}\|_2 \|\mathbf{v}\|_2}$  is the cosine similarity. Figure 2(a) displays  $\text{SimE}(\ell, t)$  as a heatmap of transformer layers against preconditioned Richardson iteration steps; the diagonal high-similarity band confirms that layer  $\ell$  tracks Richardson step  $t^*(\ell)$ , with the alignment most pronounced in the early layers. Heatmaps across all four methods and three distributions are in Figure 5.

**Best-matching step.** For each sequence  $B$  and layer  $\ell$ , we identify the iterative step  $t^*$  that maximizes cosine similarity,  $t^*(B, \ell) := \arg\max_{t \in \{0, \dots, T\}} \mathcal{C}(\mathbf{e}(\text{TF}^{(\ell)}|B), \mathbf{e}(\mathcal{A}^{(t)}|B))$ . Figure 2(b) reports the mean and single standard deviation band of  $t^*(\ell)$  computed across test sequences. A least-squares linear fit on inner layers  $\ell \in \{2, \dots, 10\}$ , excluding layer 1 (warmup) and layers 11–12 (saturation), yields  $R^2 \approx 0.976$ , indicating that each successive layer corresponds to a steady, proportional number of Richardson steps. Argmax plots for all three input distributions are in Figure 3.

## 5.2 Mechanism specificity: softmax normalization and the Gaussian kernel

The construction in Section 4 predicts that two structural ingredients are essential for the algorithmic identification: softmax row-normalization, which realizes the row-sum preconditioner  $\mathbf{D}^{-1}$ , and the Gaussian kernel structure, for which the row-sum preconditioner is well-

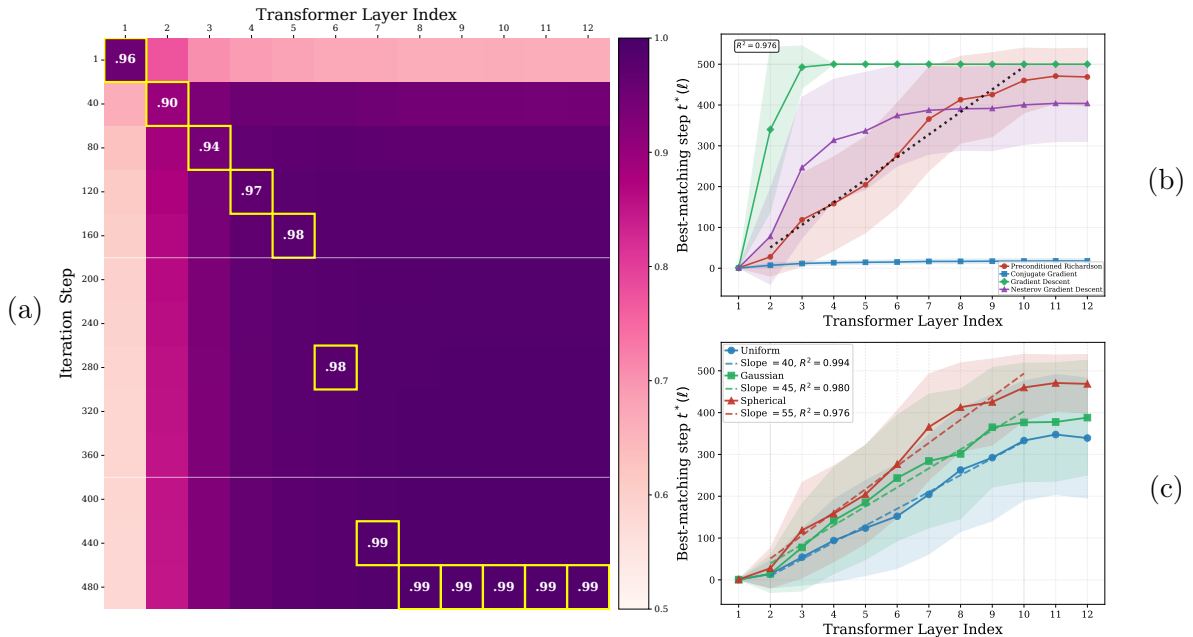


Figure 2: **Error similarity visualizations for spherical data.** (a) SimE heatmap between transformer *layer-wise* outputs and preconditioned Richardson *step-wise* outputs; yellow boxes mark the best-matching step  $t^*(\ell)$  per layer, with inset numbers denoting the peak cosine similarity. (b) Argmax trajectory  $t^*(\ell)$  for four classical algorithms; *only preconditioned Richardson exhibits a steady linear progression across the transformer’s intermediate layers*, with coefficient of determination  $R^2 = 0.976$ . (c) Best-matching Richardson steps grow approximately linearly across all three input distributions.

conditioned. Replacing either would weaken the empirical alignment.

**Linear attention.** We repeat the experiment from Section 5.1 using linear attention, i.e., raw dot-product attention without softmax. As shown in Figure 8, no single iterative method simultaneously captures both the pattern of the transformer’s error curves and the linearity of the argmax-step map. This suggests that the softmax normalization is crucial for the close connection between transformer behavior and preconditioned Richardson iterations.

**Arc-cosine-1 kernel.** We repeat the training pipeline with the Gaussian kernel replaced by the arc-cosine-1 kernel [Cho and Saul, 2009] on spherical inputs. Compared with the Gaussian kernel, the alignment with preconditioned Richardson weakens: SimE is highest for preconditioned Richardson in 11/12 layers for the Gaussian kernel but only 7/12 layers for the arc-cosine-1 kernel, and the value  $R^2$  decreases from 0.9760 to 0.9275. These results suggest that the row-sum preconditioner  $\mathbf{D} = \text{diag}(\mathbf{K}\mathbf{1})$  is aligned with the Gaussian kernel setting, and that extending the identification to non-Gaussian kernels may require a different preconditioner.

### 5.3 Architectural robustness

The construction in Section 4 uses a single attention head, depth  $\mathcal{O}(1/\epsilon)$  and MLP width  $\mathcal{O}(\sqrt{N/\epsilon})$ . We verify that the empirical preconditioned Richardson identification persists across architectural variations in head count, model width, and model depth.

**Number of heads.** We train transformers on spherical GP data with  $H \in \{1, 2, 4, 8\}$ . We then evaluate both the final-layer prediction error at  $N = 40$  and the value  $R^2$  for the argmax trajectory. As shown in Figure 9(a), both evaluations remain stable across head counts, consistent with Theorem 1 that a single head suffices to realize the relevant iterative computation.

**Model width.** We vary the model width  $d_{\text{model}} \in \{32, 64, 128, 256, 512\}$ , with  $d_{\text{ff}} = 4d_{\text{model}}$ , and measure the final-layer prediction error at  $N = 40$ . As shown in Figure 9(b), prediction error decreases rapidly with increasing width and saturates near the KRR baseline, consistent with the construction’s polynomial-in- $1/\varepsilon$  MLP-width requirement.

**Model depth.** We train 24-layer transformers on spherical GP data with bandwidths  $v = 1$  and  $v = 2$  corresponding to two condition number regimes. As shown in Figures 6 and 7, preconditioned Richardson iteration continues to align most closely with the transformer’s per-layer error trajectory across both regimes.

## 5.4 Noise-level ablation

We sweep nine test-noise levels  $\sigma_{\text{test}} \in \{10^{-3}, \dots, 1\}$  and compare the trained 12-layer transformer’s final-layer MSE at  $N = 40$  against two exact-KRR references: *Bayes-optimal* ( $\lambda = \sigma_{\text{test}}^2$ ) and *encoded* ( $\lambda = \sigma_{\text{train}}^2$ ). Across the full sweep the transformer tracks the encoded oracle rather than adapting  $\lambda$  to  $\sigma_{\text{test}}^2$ , and at  $\sigma_{\text{test}} \gg \sigma_{\text{train}}$  it sits *below* the encoded oracle (transformer-to-encoded ratio 0.77 on Spherical at  $\sigma_{\text{test}} = 1.0$ ), consistent with  $L = 12$  truncation acting as implicit early stopping. Together these findings are consistent with the transformer *behaving as if* it were running finite-depth Richardson with  $\lambda \approx \sigma_{\text{train}}^2$ . Full sweep, per-distribution curves, and numerical values are in Figure 10 and Table 3 (Appendix F.5).

## 6 Discussion

Our construction identifies softmax row-normalization with row-sum Jacobi preconditioning of the dual kernel system, showing that nonlinear in-context KRR can be implemented by an inexact preconditioned Richardson iteration: attention performs cross-token kernel matrix–vector products, while MLPs handle tokenwise scalar arithmetic. Our analysis is limited to bounded Gaussian-kernel KRR and assumes fixed  $\lambda_0$  and step size  $\eta$ , rather than prompt-adaptive solver parameters. Although Section 5.4 suggests that trained transformers behave as if using a single effective regularization parameter  $\lambda \approx \sigma_{\text{train}}^2$ , learning prompt-adaptive parameters remains open. Such an extension could connect our optimization-error analysis with sample-complexity guarantees in the style of Bai et al. [2023]. Another direction is to identify the induced solver for other shift-invariant or dot-product kernels. More broadly, since our analysis relies on the classical RKHS representer theorem, it would be interesting to ask whether analogous solver interpretations extend to Banach-space analogues [Parhi and Nowak, 2021, Bartolucci et al., 2023, Wang et al., 2024, 2025].

## Acknowledgment

M. Yan acknowledges support from an AMS-Simons travel grant. S. Tang is supported by NSF DMS CAREER Grant No. 2340631.

## References

- Kwangjun Ahn, Xiang Cheng, Hadi Daneshmand, and Suvrit Sra. Transformers learn to implement preconditioned gradient descent for in-context learning. In *Advances in Neural Information Processing Systems*, volume 36, pages 45614–45650, 2023. [1](#), [2](#), [5.1](#)
- Ekin Akyürek, Dale Schuurmans, Jacob Andreas, Tengyu Ma, and Denny Zhou. What learning algorithm is in-context learning? investigations with linear models. In *The Eleventh International Conference on Learning Representations*, 2023. [1](#), [2](#), [5.1](#)
- Ekin Akyürek, Bailin Wang, Yoon Kim, and Jacob Andreas. In-context language learning: Architectures and algorithms. In *International Conference on Machine Learning*. PMLR, 2024. [2](#)
- Francis Bach. Breaking the curse of dimensionality with convex neural networks. *Journal of Machine Learning Research*, 18(19):1–53, 2017. [4](#), [B](#)
- Francis Bach. *Learning Theory from First Principles*. MIT Press, 2024. [D](#)
- Yu Bai, Fan Chen, Huan Wang, Caiming Xiong, and Song Mei. Transformers as statisticians: Provable in-context learning with in-context algorithm selection. In *Advances in Neural Information Processing Systems*, volume 36, pages 57125–57211, 2023. [1](#), [2](#), [3.2](#), [4](#), [6](#), [B](#), [E](#)
- Francesca Bartolucci, Ernesto De Vito, Lorenzo Rosasco, and Stefano Vigogna. Understanding neural networks with reproducing kernel Banach spaces. *Applied and Computational Harmonic Analysis*, 62:194–236, 2023. [6](#)
- Satwik Bhattamishra, Arkil Patel, Phil Blunsom, and Varun Kanade. Understanding in-context learning in transformers and LLMs by learning to learn discrete functions. In *International Conference on Learning Representations*, 2024. [2](#)
- Tom Brown, Benjamin Mann, Nick Ryder, Melanie Subbiah, Jared D Kaplan, Prafulla Dhariwal, Arvind Neelakantan, Pranav Shyam, Girish Sastry, Amanda Askell, et al. Language models are few-shot learners. In *Advances in Neural Information Processing Systems*, volume 33, pages 1877–1901, 2020. [1](#)
- Andrea Caponnetto and Ernesto De Vito. Optimal rates for the regularized least-squares algorithm. *Foundations of Computational Mathematics*, 7(3):331–368, 2007. [3.2](#)
- Siyu Chen, Heejune Sheen, Tianhao Wang, and Zhuoran Yang. Training dynamics of multi-head softmax attention for in-context learning: Emergence, convergence, and optimality. In *The Thirty Seventh Annual Conference on Learning Theory*, volume 247, pages 4573–4573. PMLR, 2024. [2](#)
- Xiang Cheng, Yuxin Chen, and Suvrit Sra. Transformers implement functional gradient descent to learn non-linear functions in context. In *International Conference on Machine Learning*, volume 235, pages 8002–8037. PMLR, 2024. [1](#), [2](#)
- Youngmin Cho and Lawrence K. Saul. Kernel methods for deep learning. In *Advances in Neural Information Processing Systems 22*, 2009. [5.2](#)
- Liam Collins, Advait Parulekar, Aryan Mokhtari, Sujay Sanghavi, and Sanjay Shakkottai. In-context learning with transformers: Softmax attention adapts to function lipschitzness. In *Advances in Neural Information Processing Systems*, volume 37, pages 92638–92696, 2024. [2](#)

- Carl De Boor. *A practical guide to splines*, volume 27. springer New York, 1978. 4, B, B, B
- Samet Demir and Zafer Dogan. Asymptotic study of in-context learning with random transformers through equivalent models, 2025. 2
- Ronald DeVore. Nonlinear approximation. *Acta numerica*, 7:51–150, 1998. 4, B
- Ronald DeVore, Boris Hanin, and Guergana Petrova. Neural network approximation. *Acta Numerica*, 30:327–444, 2021. 4, B
- Sara Dragutinović, Andrew M. Saxe, and Aaditya K. Singh. Softmax  $\geq$  linear: Transformers may learn to classify in-context by kernel gradient descent. *arXiv preprint arXiv:2510.10425*, 2025. 1, 2, 3.2
- Deqing Fu, Tian-Qi Chen, Robin Jia, and Vatsal Sharan. Transformers learn to achieve second-order convergence rates for in-context linear regression. In *Advances in Neural Information Processing Systems*, volume 37, pages 98675–98716, 2024. 1, 2, 3.2, 5.1, E
- Shivam Garg, Dimitris Tsipras, Percy S. Liang, and Gregory Valiant. What can transformers learn in-context? a case study of simple function classes. In *Advances in Neural Information Processing Systems*, volume 35, pages 30583–30598, 2022. 1, 2, 5
- Chi Han, Ziqi Wang, Han Zhao, and Heng Ji. Understanding emergent in-context learning from a kernel regression perspective. *Transactions on Machine Learning Research*, 2025. 1, 2
- Yu Huang, Yuan Cheng, and Yingbin Liang. In-context convergence of transformers. In *Proceedings of the 41st International Conference on Machine Learning*, volume 235, pages 19660–19722. PMLR, 2024. 2
- Zihao Li, Yuan Cao, Cheng Gao, Yihang He, Han Liu, Jason M. Klusowski, Jianqing Fan, and Mengdi Wang. One-layer transformer provably learns one-nearest neighbor in context. In *Advances in Neural Information Processing Systems*, volume 37, pages 82166–82204, 2024. 2
- Yue M. Lu, Mary I. Letey, Jacob A. Zavatone-Veth, Anindita Maiti, and Cengiz Pehlevan. Asymptotic theory of in-context learning by linear attention. *Proceedings of the National Academy of Sciences*, 122(28):e2502599122, 2025. 2
- Arvind V. Mahankali, Tatsunori B. Hashimoto, and Tengyu Ma. One step of gradient descent is provably the optimal in-context learner with one layer of linear self-attention. In *International Conference on Learning Representations*, 2024. 1, 2, 5.1
- Rahul Parhi and Robert D Nowak. Banach space representer theorems for neural networks and ridge splines. *Journal of Machine Learning Research*, 22(43):1–40, 2021. 6
- Alec Radford, Jeffrey Wu, Rewon Child, David Luan, Dario Amodei, and Ilya Sutskever. Language models are unsupervised multitask learners. *OpenAI Blog*, 2019. 5
- Carl Edward Rasmussen and Christopher K. I. Williams. *Gaussian Processes for Machine Learning*. MIT Press, 2006. 3.2
- Victor Ryaben’kii and Semyon Tsynkov. *A Theoretical Introduction to Numerical Analysis*. Chapman & Hall, 2006. D
- Michael E Sander and Gabriel Peyré. Towards understanding the universality of transformers for next-token prediction. *arXiv preprint arXiv:2410.03011*, 2024. 1

- Bernhard Schölkopf, Ralf Herbrich, and Alex J Smola. A generalized representer theorem. In *International conference on computational learning theory*, pages 416–426. Springer, 2001. [3.2](#)
- Zhaiming Shen, Alexander Hsu, Rongjie Lai, and Wenjing Liao. Understanding in-context learning on structured manifolds: Bridging attention to kernel methods. *arXiv preprint arXiv:2506.10959*, 2025. [2](#)
- Jonathan R Shewchuk. An introduction to the conjugate gradient method without the agonizing pain. 1994. [D](#)
- Haoyuan Sun, Ali Jadbabaie, and Navid Azizan. On the role of transformer feed-forward layers in nonlinear in-context learning, 2025. [2](#)
- Hugo Touvron, Thibaut Lavril, Gautier Izacard, Xavier Martinet, Marie-Anne Lachaux, Timothée Lacroix, Baptiste Rozière, Naman Goyal, Eric Hambro, Faisal Azhar, et al. Llama: Open and efficient foundation language models. *arXiv preprint arXiv:2302.13971*, 2023. [3.2](#)
- Ashish Vaswani, Noam Shazeer, Niki Parmar, Jakob Uszkoreit, Llion Jones, Aidan N Gomez, Łukasz Kaiser, and Illia Polosukhin. Attention is all you need. *Advances in neural information processing systems*, 30, 2017. [3.1](#)
- Max Vladymyrov, Johannes von Oswald, Mark Sandler, and Rong Ge. Linear transformers are versatile in-context learners. In *Advances in Neural Information Processing Systems*, volume 37, pages 48784–48809, 2024. [1](#), [2](#)
- Johannes von Oswald, Eyvind Niklasson, Ettore Randazzo, João Sacramento, Alexander Mordvintsev, Andrey Zhmoginov, and Max Vladymyrov. Transformers learn in-context by gradient descent. In *International Conference on Machine Learning*, pages 35151–35174. PMLR, 2023. [1](#), [2](#), [3.2](#), [5.1](#)
- Rui Wang, Yuesheng Xu, and Mingsong Yan. Sparse representer theorems for learning in reproducing kernel Banach spaces. *Journal of Machine Learning Research*, 25(93):1–45, 2024. [6](#)
- Rui Wang, Yuesheng Xu, and Mingsong Yan. Hypothesis spaces for deep learning. *Neural Networks*, page 107995, 2025. [6](#)
- Ruiqi Zhang, Spencer Frei, and Peter L. Bartlett. Trained transformers learn linear models in-context. *Journal of Machine Learning Research*, 25(49):1–55, 2024a. [2](#)
- Ruiqi Zhang, Jingfeng Wu, and Peter L. Bartlett. In-context learning of a linear transformer block: Benefits of the MLP component and one-step GD initialization. In *Advances in Neural Information Processing Systems*, volume 37, pages 18310–18361, 2024b. [2](#)
- Yedi Zhang, Freya Behrens, Florent Krzakala, and Lenka Zdeborová. Training dynamics of in-context learning in linear attention. *arXiv preprint arXiv:2501.16265*, 2025. [1](#), [2](#)

## A Error Analysis of Inexact Preconditioned Richardson Iterations

In this section, we present an error analysis of the inexact preconditioned Richardson iteration, an algorithm we will subsequently implement via a specifically constructed transformer. We proceed with a helpful lemma.

**Lemma 2.** *Let  $\lambda_0 > 0$  and  $\lambda = \lambda_0 N$ . Suppose that  $\mathbf{w}^* = [w_i^* : i \in [N]]$  is the solution of linear system (2). Then it holds that*

$$\|\mathbf{K}\mathbf{w}^*\|_\infty \leq \frac{B_y}{\sqrt{\lambda_0}}, \quad \|\mathbf{w}^*\|_\infty \leq \frac{\left(\frac{1}{\sqrt{\lambda_0}} + 1\right) B_y}{\lambda_0} \frac{1}{N}.$$

*Proof.* It is known by representer theorem that  $f^*(x) = \sum_{i=1}^N w_i^* \mathcal{K}(\mathbf{x}_i, \cdot)$  is the optimal solution of (1). We denote  $\mathcal{L}(f) := \frac{1}{N} \sum_{i \in [N]} (f(\mathbf{x}_i) - y_i)^2 + \lambda_0 \|f\|_{\mathcal{H}}^2$ . The optimality of  $f^*$  implies

$$\lambda_0 \|f^*\|_{\mathcal{H}}^2 \leq \mathcal{L}(f^*) \leq \mathcal{L}(0) = \frac{1}{N} \sum_{i=1}^N y_i^2 \leq B_y^2,$$

and hence  $\|f^*\|_{\mathcal{H}} \leq \frac{B_y}{\sqrt{\lambda_0}}$ . By the reproducing property in RKHS, i.e.,  $f^*(\mathbf{x}) = \langle f^*, \mathcal{K}(\mathbf{x}, \cdot) \rangle_{\mathcal{H}}$ , we get that

$$|f^*(\mathbf{x})| \leq \|f^*\|_{\mathcal{H}} \|\mathcal{K}(\mathbf{x}, \cdot)\|_{\mathcal{H}} = \|f^*\|_{\mathcal{H}} \sqrt{\mathcal{K}(\mathbf{x}, \mathbf{x})} \leq \frac{B_y}{\sqrt{\lambda_0}}, \quad \text{for all } \mathbf{x} \in \mathbb{R}^d.$$

Note that  $\mathbf{K}\mathbf{w}^* = [f^*(\mathbf{x}_i) : i \in [N]]$ . Consequently, we obtain from the previous estimate that

$$\|\mathbf{K}\mathbf{w}^*\|_\infty = \max_{i \in [N]} |f^*(\mathbf{x}_i)| \leq \frac{B_y}{\sqrt{\lambda_0}}.$$

Moreover, from the linear system (2), we get

$$\|\mathbf{w}^*\|_\infty = \frac{\|\mathbf{K}\mathbf{w}^* - \mathbf{y}\|_\infty}{\lambda} \leq \frac{\|\mathbf{K}\mathbf{w}^*\|_\infty + \|\mathbf{y}\|_\infty}{\lambda} \leq \frac{\left(\frac{1}{\sqrt{\lambda_0}} + 1\right) B_y}{\lambda_0} \frac{1}{N}.$$

This completes the proof.  $\square$

We recall that the bounded data assumption (i.e.,  $\|\mathbf{x}_i\|_2 \leq B_x$  for all samples  $\mathbf{x}_i$ ) and boundedness of the Gaussian kernel imply that for all  $i \in [N]$ ,

$$N\kappa_{\min} \leq \sum_{j \in [N]} \mathcal{K}(\mathbf{x}_i, \mathbf{x}_j) \leq N \quad (4)$$

where  $\kappa_{\min} := \exp\left(-\frac{2B_x^2}{v^2}\right)$ .

**Theorem 3** (Error Analysis for Inexact Preconditioned Richardson Iterations). *Suppose that the bounded data assumption holds with constants  $B_x$  and  $B_y$ . Let initial value  $\mathbf{w}^{(0)} = \mathbf{0}$ . Let  $\epsilon_{\text{flip}}, \epsilon_{\text{sq}}, \tilde{\epsilon}_{\text{sq}} \in (0, 1)$ . Let  $\lambda_0, \eta > 0$  and  $\lambda = \lambda_0 N$ . Consider inexact preconditioned Richardson iteration*

$$\mathbf{w}^{(\ell+1)} = \mathbf{w}^{(\ell)} + \eta \left( \mathbf{D}^{-1} \mathbf{y} - \mathbf{D}^{-1} (\mathbf{K} + \lambda \mathbf{I}) \mathbf{w}^{(\ell)} \right) + \eta \left( \left( \mathbf{y} - \lambda \mathbf{w}^{(\ell)} \right) \odot \mathbf{r} + \frac{\tau_+ - \tau_- - \lambda \tilde{\tau}_+^{(\ell)} + \lambda \tilde{\tau}_-^{(\ell)}}{4} \right), \quad (5)$$

with

$$\|\mathbf{r}\|_\infty \leq \frac{\epsilon_{\text{flip}}}{N}, \quad \|\boldsymbol{\tau}_+\|_\infty, \|\boldsymbol{\tau}_-\|_\infty \leq \frac{\epsilon_{\text{sq}}}{N}, \quad \|\tilde{\boldsymbol{\tau}}_+^{(\ell)}\|_\infty, \|\tilde{\boldsymbol{\tau}}_-^{(\ell)}\|_\infty \leq \frac{\tilde{\epsilon}_{\text{sq}}}{N^2}. \quad (6)$$

Then it holds that

$$\sqrt{N} \left\| \mathbf{w}^{(\ell)} - \mathbf{w}^* \right\|_2 \leq \|\mathbf{A}\|_{2 \rightarrow 2}^\ell \frac{\left(\frac{1}{\sqrt{\lambda_0}} + 1\right) B_y}{\lambda_0 \sqrt{\kappa_{\min}}} + \frac{\eta \left( \frac{B_y}{\sqrt{\lambda_0}} \epsilon_{\text{flip}} + (1 + \lambda_0) (\epsilon_{\text{sq}} + \tilde{\epsilon}_{\text{sq}}) \right)}{(1 - \|\mathbf{A}\|_{2 \rightarrow 2}) \sqrt{\kappa_{\min}}}, \quad (7)$$

where

$$\mathbf{A} := \mathbf{I} - \eta \left( \lambda \text{diag}(\mathbf{r}) + \mathbf{D}^{-1/2} (\mathbf{K} + \lambda \mathbf{I}) \mathbf{D}^{-1/2} \right). \quad (8)$$

*Proof.* We subtract  $\mathbf{w}^*$  for both sides of (5), and note that the exact solution  $\mathbf{w}^*$  satisfies  $(\mathbf{K} + \lambda \mathbf{I})\mathbf{w}^* = \mathbf{y}$ , then

$$\begin{aligned} \mathbf{w}^{(\ell+1)} - \mathbf{w}^* &= \mathbf{w}^{(\ell)} - \mathbf{w}^* + \eta \mathbf{D}^{-1} (\mathbf{K} + \lambda \mathbf{I}) (\mathbf{w}^* - \mathbf{w}^{(\ell)}) + \eta \left( ((\mathbf{K} + \lambda \mathbf{I})\mathbf{w}^* - \lambda \mathbf{w}^{(\ell)}) \odot \mathbf{r} + \boldsymbol{\Delta}^{(\ell)} \right) \\ &= (\mathbf{I} - \eta (\lambda \text{diag}(\mathbf{r}) + \mathbf{D}^{-1} (\mathbf{K} + \lambda \mathbf{I}))) (\mathbf{w}^{(\ell)} - \mathbf{w}^*) + \eta \left( (\mathbf{K} \mathbf{w}^*) \odot \mathbf{r} + \boldsymbol{\Delta}^{(\ell)} \right) \end{aligned} \quad (9)$$

where

$$\boldsymbol{\Delta}^{(\ell)} := \frac{\boldsymbol{\tau}_+ - \boldsymbol{\tau}_- - \lambda \tilde{\boldsymbol{\tau}}_+^{(\ell)} + \lambda \tilde{\boldsymbol{\tau}}_-^{(\ell)}}{4}.$$

Note that

$$\begin{aligned} \mathbf{I} - \eta (\lambda \text{diag}(\mathbf{r}) + \mathbf{D}^{-1} (\mathbf{K} + \lambda \mathbf{I})) &= \mathbf{D}^{-1/2} \left( \mathbf{I} - \eta (\lambda \text{diag}(\mathbf{r}) + \mathbf{D}^{-1/2} (\mathbf{K} + \lambda \mathbf{I}) \mathbf{D}^{-1/2}) \right) \mathbf{D}^{1/2}, \\ &= \mathbf{D}^{-1/2} \mathbf{A} \mathbf{D}^{1/2}. \end{aligned}$$

This, combined with (9), implies

$$\mathbf{D}^{1/2} (\mathbf{w}^{(\ell+1)} - \mathbf{w}^*) = \underbrace{\mathbf{A} \mathbf{D}^{1/2} (\mathbf{w}^{(\ell)} - \mathbf{w}^*)}_{\text{denoted by } \mathbf{e}^{(\ell)}} + \underbrace{\mathbf{D}^{1/2} \eta \left( (\mathbf{K} \mathbf{w}^*) \odot \mathbf{r} + \boldsymbol{\Delta}^{(\ell)} \right)}_{\text{denoted by } \boldsymbol{\epsilon}^{(\ell)}}.$$

We rewrite the above equation as  $\mathbf{e}^{(\ell+1)} = \mathbf{A} \mathbf{e}^{(\ell)} + \boldsymbol{\epsilon}^{(\ell)}$ , which with an argument of recursion gives

$$\mathbf{e}^{(\ell+1)} = \mathbf{A}^{\ell+1} \mathbf{e}^{(0)} + \sum_{j=0}^{\ell} \mathbf{A}^j \boldsymbol{\epsilon}^{(\ell-j)}. \quad (10)$$

By definition of  $\boldsymbol{\epsilon}^{(\ell)}$ , we have

$$\left\| \boldsymbol{\epsilon}^{(\ell)} \right\|_2 \leq \sqrt{N} \left\| \boldsymbol{\epsilon}^{(\ell)} \right\|_\infty \leq \sqrt{N} \eta \left\| \text{diag}(\mathbf{D}^{1/2}) \right\|_\infty \left( \|\mathbf{K} \mathbf{w}^*\|_\infty \|\mathbf{r}\|_\infty + \left\| \boldsymbol{\Delta}^{(\ell)} \right\|_\infty \right).$$

Recall that (4) implies  $\left\| \text{diag}(\mathbf{D}^{1/2}) \right\|_\infty \leq \sqrt{N}$ ; Lemma 2 yields  $\|\mathbf{K} \mathbf{w}^*\|_\infty \leq B_y / \sqrt{\lambda_0}$ ; assumption (6) yields  $\|\mathbf{r}\|_\infty \leq \epsilon_{\text{flip}} / N$  and

$$\left\| \boldsymbol{\Delta}^{(\ell)} \right\|_\infty \leq \frac{\|\boldsymbol{\tau}_+\|_\infty + \|\boldsymbol{\tau}_-\|_\infty + \lambda (\|\tilde{\boldsymbol{\tau}}_+\|_\infty + \|\tilde{\boldsymbol{\tau}}_-\|_\infty)}{4} \leq \frac{\epsilon_{\text{sq}} + \lambda_0 \tilde{\epsilon}_{\text{sq}}}{2N} \leq \frac{(1 + \lambda_0) (\epsilon_{\text{sq}} + \tilde{\epsilon}_{\text{sq}})}{N}.$$

Consequently, we have

$$\left\| \boldsymbol{\epsilon}^{(\ell)} \right\|_2 \leq \eta \left( \frac{B_y}{\sqrt{\lambda_0}} \epsilon_{\text{flip}} + (1 + \lambda_0) (\epsilon_{\text{sq}} + \tilde{\epsilon}_{\text{sq}}) \right) \equiv B_\epsilon.$$

Therefore, for all  $\ell$ , we obtain from (10) that

$$\left\| \mathbf{e}^{(\ell)} \right\|_2 \leq \|\mathbf{A}\|_{2 \rightarrow 2}^\ell \left\| \mathbf{e}^{(0)} \right\|_2 + B_\epsilon \sum_{j=0}^{\ell-1} \|\mathbf{A}\|_{2 \rightarrow 2}^j \leq \|\mathbf{A}\|_{2 \rightarrow 2}^\ell \left\| \mathbf{e}^{(0)} \right\|_2 + \frac{B_\epsilon}{1 - \|\mathbf{A}\|_{2 \rightarrow 2}}.$$

Note that by (4), we have

$$\left\| \mathbf{e}^{(\ell)} \right\|_2 = \left\| \mathbf{D}^{1/2} \left( \mathbf{w}^{(\ell)} - \mathbf{w}^* \right) \right\|_2 \geq \sqrt{\kappa_{\min} N} \left\| \mathbf{w}^{(\ell)} - \mathbf{w}^* \right\|_2,$$

and by Lemma 2, we have

$$\left\| \mathbf{e}^{(0)} \right\|_2 = \left\| \mathbf{D}^{1/2} \left( \mathbf{w}^{(0)} - \mathbf{w}^* \right) \right\|_2 = \left\| \mathbf{D}^{1/2} \mathbf{w}^* \right\|_2 \leq N \|\mathbf{w}^*\|_\infty \leq \frac{\left( \frac{1}{\sqrt{\lambda_0}} + 1 \right) B_y}{\lambda_0}$$

which combining with the previous estimate yields (7).  $\square$

**Lemma 4** (Estimate of  $\|\mathbf{A}\|_{2 \rightarrow 2}$ ). *Under conditions of Theorem 3, let  $\mathbf{A}$  be defined in (8). If*

$$0 < \eta < \frac{1}{\lambda_0 \epsilon_{\text{flip}} + 1 + \lambda_0 / \kappa_{\min}}, \quad (11)$$

then it holds that

$$\|\mathbf{A}\|_{2 \rightarrow 2} < 1 - \eta \lambda_0 (1 - \epsilon_{\text{flip}}) \in (0, 1).$$

*Proof.* We denote  $\mathbf{K}_\lambda := \lambda \text{diag}(\mathbf{r}) + \mathbf{D}^{-1/2} (\mathbf{K} + \lambda \mathbf{I}) \mathbf{D}^{-1/2}$ . Then the matrix  $\mathbf{A}$  can be rewritten as  $\mathbf{A} = \mathbf{I} - \eta \mathbf{K}_\lambda$ . Since  $\mathbf{A}$  is symmetric,  $\|\mathbf{A}\|_{2 \rightarrow 2}$  equals its maximum absolute eigenvalue. Note that the eigenvalues of  $\mathbf{A}$  satisfy

$$\text{eig}(\mathbf{A}) = 1 - \eta \text{eig}(\mathbf{K}_\lambda).$$

By Weyl's inequality, the maximum eigenvalue of  $\mathbf{K}_\lambda$  is bounded by

$$\begin{aligned} \text{eig}_{\max}(\mathbf{K}_\lambda) &\leq \text{eig}_{\max}(\lambda \text{diag}(\mathbf{r})) + \text{eig}_{\max}(\mathbf{D}^{-1/2} \mathbf{K} \mathbf{D}^{-1/2}) + \text{eig}_{\max}(\lambda \mathbf{D}^{-1}) \\ &\leq \lambda_0 \epsilon_{\text{flip}} + 1 + \frac{\lambda_0}{\kappa_{\min}}, \end{aligned} \quad (12)$$

where we used assumption (6), relation (4),  $\lambda = \lambda_0 N$  and  $\text{eig}_{\max}(\mathbf{D}^{-1/2} \mathbf{K} \mathbf{D}^{-1/2}) \leq 1$ . Assumption (11) of  $\eta$  guarantees  $\eta \text{eig}_{\max}(\mathbf{K}_\lambda) < 1$ . Consequently, all eigenvalues of  $\mathbf{A}$  are strictly positive, i.e.,

$$\text{eig}_{\min}(\mathbf{A}) = 1 - \eta \text{eig}_{\max}(\mathbf{K}_\lambda) > 0.$$

It follows that the operator norm of  $\mathbf{A}$  is exactly its maximum eigenvalue. Hence,

$$\|\mathbf{A}\|_{2 \rightarrow 2} = \text{eig}_{\max}(\mathbf{A}) = 1 - \eta \text{eig}_{\min}(\mathbf{K}_\lambda).$$

Applying Weyl's inequality to the minimum eigenvalue gives

$$\text{eig}_{\min}(\mathbf{K}_\lambda) \geq \text{eig}_{\min}(\lambda \text{diag}(\mathbf{r})) + \text{eig}_{\min}(\mathbf{D}^{-1/2} \mathbf{K} \mathbf{D}^{-1/2}) + \text{eig}_{\min}(\lambda \mathbf{D}^{-1}) > -\lambda_0 \epsilon_{\text{flip}} + \lambda_0, \quad (13)$$

where we used assumption (6), relation (4),  $\lambda = \lambda_0 N$  and the fact that matrix  $\mathbf{D}^{-1/2} \mathbf{K} \mathbf{D}^{-1/2}$  is positive definite. Therefore, the operator norm is bounded as

$$\|\mathbf{A}\|_{2 \rightarrow 2} < 1 - \eta \lambda_0 (1 - \epsilon_{\text{flip}}).$$

We finally verify the upper bound  $1 - \eta \lambda_0 (1 - \epsilon_{\text{flip}})$  is in  $(0, 1)$ . It suffices to show that

$$\eta \lambda_0 (1 - \epsilon_{\text{flip}}) \in (0, 1). \quad (14)$$

We obtain from (12) and (13) that  $\lambda_0 (1 - \epsilon_{\text{flip}}) < \lambda_0 \epsilon_{\text{flip}} + 1 + \frac{\lambda_0}{\kappa_{\min}}$ , and hence (14) is clearly true due to assumption (11) for  $\eta$ .  $\square$

**Theorem 5** (Entry-wise boundedness of  $\mathbf{w}^{(\ell)}$ ). *Suppose that the bounded data assumption holds with constants  $B_x$  and  $B_y$ . Let initial value  $\mathbf{w}^{(0)} = \mathbf{0}$ . Let  $\epsilon_{\text{sq}}, \tilde{\epsilon}_{\text{sq}} \in (0, 1)$  and  $\epsilon_{\text{flip}} \in (0, c)$  for a constant  $c \in (0, 1)$ . Let  $\lambda_0 > 0$  and  $\eta$  satisfy (11). Let  $\mathbf{w}^{(\ell)}$  be generated from inexact preconditioned Richardson iteration (5) with condition (6). Then for all  $\ell \in \mathbb{N}$ ,*

$$\left\| \mathbf{w}^{(\ell)} \right\|_{\infty} \leq B_w := \frac{1}{\sqrt{N}} \left( \frac{\left( \frac{1}{\sqrt{\lambda_0}} + 1 \right) B_y}{\lambda_0 \sqrt{\kappa_{\min}}} + \frac{\frac{B_y}{\sqrt{\lambda_0}} + 2(1 + \lambda_0)}{\lambda_0 (1 - c) \sqrt{\kappa_{\min}}} \right) + \frac{1}{N} \left( \frac{\left( \frac{1}{\sqrt{\lambda_0}} + 1 \right) B_y}{\lambda_0} \right). \quad (15)$$

*Proof.* We obtain from Theorem 3 that

$$\left\| \mathbf{w}^{(\ell)} - \mathbf{w}^* \right\|_{\infty} \leq \left\| \mathbf{w}^{(\ell)} - \mathbf{w}^* \right\|_2 \leq \frac{1}{\sqrt{N}} \left( \left\| \mathbf{A} \right\|_{2 \rightarrow 2}^{\ell} \frac{\left( \frac{1}{\sqrt{\lambda_0}} + 1 \right) B_y}{\lambda_0 \sqrt{\kappa_{\min}}} + \frac{\eta \left( \frac{B_y}{\sqrt{\lambda_0}} + 2(1 + \lambda_0) \right)}{(1 - \left\| \mathbf{A} \right\|_{2 \rightarrow 2}) \sqrt{\kappa_{\min}}} \right),$$

where we used assumptions of  $\epsilon_{\text{flip}}, \epsilon_{\text{sq}}, \tilde{\epsilon}_{\text{sq}} < 1$ . Furthermore, by Lemma 4, we apply the estimate of  $\left\| \mathbf{A} \right\|_{2 \rightarrow 2}$  and get

$$\left\| \mathbf{w}^{(\ell)} - \mathbf{w}^* \right\|_{\infty} \leq \frac{1}{\sqrt{N}} \left( \frac{\left( \frac{1}{\sqrt{\lambda_0}} + 1 \right) B_y}{\lambda_0 \sqrt{\kappa_{\min}}} + \frac{\frac{B_y}{\sqrt{\lambda_0}} + 2(1 + \lambda_0)}{\lambda_0 (1 - c) \sqrt{\kappa_{\min}}} \right),$$

where we used the assumption of  $\epsilon_{\text{flip}} < c$ . The desired result (15) can be immediately obtained by the triangle inequality  $\left\| \mathbf{w}^{(\ell)} \right\|_{\infty} \leq \left\| \mathbf{w}^{(\ell)} - \mathbf{w}^* \right\|_{\infty} + \left\| \mathbf{w}^* \right\|_{\infty}$  and estimate of  $\left\| \mathbf{w}^* \right\|_{\infty}$  established in Lemma 2.  $\square$

**Proposition 6.** *Suppose that assumptions of Theorem 5 hold and  $\mathbf{w}^* = [w_i^* : i \in [N]]$  is the solution of linear system (2). Then for all  $\ell \in \mathbb{N}$ , it holds that*

$$\left| \sum_{i=1}^N \left( w_i^{(\ell)} - w_i^* \right) \mathcal{K}(\mathbf{x}_i, \mathbf{x}_{N+1}) \right| \leq (1 - \eta \lambda_0 (1 - c))^{\ell} \frac{\left( \frac{1}{\sqrt{\lambda_0}} + 1 \right) B_y}{\lambda_0 \sqrt{\kappa_{\min}}} + \frac{\frac{B_y}{\sqrt{\lambda_0}} \epsilon_{\text{flip}} + (1 + \lambda_0) (\epsilon_{\text{sq}} + \tilde{\epsilon}_{\text{sq}})}{\lambda_0 (1 - c) \sqrt{\kappa_{\min}}}.$$

*Proof.* By the Cauchy-Schwarz inequality,

$$\left| \sum_{i=1}^N \left( w_i^{(\ell)} - w_i^* \right) \mathcal{K}(\mathbf{x}_i, \mathbf{x}_{N+1}) \right| \leq \left\| \mathbf{w}^{(\ell)} - \mathbf{w}^* \right\|_2 \left( \sum_{i=1}^N (\mathcal{K}(\mathbf{x}_i, \mathbf{x}_{N+1}))^2 \right)^{\frac{1}{2}} \leq \sqrt{N} \left\| \mathbf{w}^{(\ell)} - \mathbf{w}^* \right\|_2.$$

Moreover, it follows from Theorem 3 and Lemma 4 that

$$\sqrt{N} \left\| \mathbf{w}^{(\ell)} - \mathbf{w}^* \right\|_2 \leq (1 - \eta \lambda_0 (1 - c))^{\ell} \frac{\left( \frac{1}{\sqrt{\lambda_0}} + 1 \right) B_y}{\lambda_0 \sqrt{\kappa_{\min}}} + \frac{\frac{B_y}{\sqrt{\lambda_0}} \epsilon_{\text{flip}} + (1 + \lambda_0) (\epsilon_{\text{sq}} + \tilde{\epsilon}_{\text{sq}})}{\lambda_0 (1 - c) \sqrt{\kappa_{\min}}}.$$

The desired result immediately follows from the above estimates.  $\square$

## B Approximation Power of Single-Layer ReLU Networks

In the construction of Transformers for in-context learning, we typically use the MLP layer (a single-layer ReLU neural network) to approximate necessary arithmetic operations. For general dimension-free approximation (which holds for arbitrary input dimensions), achieving a target accuracy of  $\epsilon$  requires a network width that scales as  $\mathcal{O}(\log(1/\epsilon)/\epsilon^2)$  [Bach, 2017, Bai et al., 2023]. While broadly applicable, these existential guarantees are inherently non-constructive and

suffer from a relatively loose dependence on the error tolerance. However, because the specific operations we need to approximate are strictly one-dimensional smooth functions, we can use continuous piecewise-linear splines to reduce this width requirement to  $\mathcal{O}(1/\sqrt{\epsilon})$  [De Boor, 1978, DeVore et al., 2021, DeVore, 1998]. Furthermore, unlike dimension-free approaches, spline-based methods provide an explicit mathematical recipe for constructing the exact neural parameters. Therefore, in this section, we adopt these constructive spline arguments to establish sharper, explicitly realizable network width bounds.

To explicitly control the approximation error, we present the following constructive lemma. This result follows directly from standard error analysis of piecewise linear interpolation and well-known ReLU representations of splines [De Boor, 1978, DeVore et al., 2021]. We state it here in the form required for our theoretical constructions and omit the standard proof.

**Lemma 7** (Constructive Approximation of Single-layer ReLU network). *Let  $f \in C^2[M_1, M_2]$  and let  $M_1 = x_0 < x_1 < \dots < x_n = M_2$  be an arbitrary partition of  $[M_1, M_2]$  with  $n \in \mathbb{N}$ . We define the network parameters explicitly as follows:*

$$d = f(M_1), \quad a_s = 1, \quad b_s = -x_{s-1}, \quad \text{for } s = 1, \dots, n,$$

$$c_s = \begin{cases} \frac{f(x_1) - f(x_0)}{x_1 - x_0}, & s = 1, \\ \frac{f(x_s) - f(x_{s-1})}{x_s - x_{s-1}} - \frac{f(x_{s-1}) - f(x_{s-2})}{x_{s-1} - x_{s-2}}, & s = 2, \dots, n. \end{cases}$$

Then the neural network  $\phi(x) = \sum_{s=1}^n c_s \text{ReLU}(a_s x + b_s) + d$  satisfies the uniform approximation bound

$$\sup_{x \in [M_1, M_2]} |f(x) - \phi(x)| \leq \frac{1}{8} \max_{k \in [n]} \left( (x_k - x_{k-1})^2 \sup_{x \in [x_{k-1}, x_k]} |f''(x)| \right).$$

We now apply the general bound from Lemma 7 to derive explicit network widths for approximating specific one-dimensional smooth functions. Because our transformer blocks rely on these functions to compute intermediate variables, we formulate their approximation bounds as direct corollaries below.

**Corollary 8** (Approximation of  $x^2$  on  $[-\delta, \delta]$ ). *Let  $\delta > 0$  and target accuracy  $\epsilon > 0$ . If the network width  $n \in \mathbb{N}$  satisfies  $n \geq \delta/\sqrt{\epsilon}$ , then there exist parameters  $a_s, b_s, c_s \in \mathbb{R}$  for  $s \in [n]$ , and  $d \in \mathbb{R}$ , such that the neural network  $\phi(x) = \sum_{s=1}^n c_s \text{ReLU}(a_s x + b_s) + d$  satisfies the uniform bound  $\sup_{x \in [-\delta, \delta]} |x^2 - \phi(x)| \leq \epsilon$ .*

*Proof.* We apply Lemma 7 using a uniform partition  $x_k = -\delta + 2\delta k/n$ . The interval width is constantly  $2\delta/n$ . Because  $f''(x) = 2$ , the error bound becomes  $\frac{1}{8}(4\delta^2/n^2)(2) = \delta^2/n^2$ . Enforcing  $\delta^2/n^2 \leq \epsilon$  yields the condition on  $n$ .  $\square$

**Corollary 9** (Approximation of  $x/(1-x)$  on  $[0, \delta]$ ). *Let  $\delta \in (0, 1)$  and target accuracy  $\epsilon \in (0, 1)$ . If the network width  $n \in \mathbb{N}$  satisfies*

$$n \geq \frac{2((1-\delta)^{-1/2} - 1)}{\sqrt{\epsilon}} = \mathcal{O}(1/\sqrt{\epsilon(1-\delta)}),$$

then there exist parameters  $a_s, b_s, c_s \in \mathbb{R}$  for  $s \in [n]$ , and  $d \in \mathbb{R}$ , such that the neural network  $\phi(x) = \sum_{s=1}^n c_s \text{ReLU}(a_s x + b_s) + d$  satisfies  $\sup_{x \in [0, \delta]} \left| \frac{x}{1-x} - \phi(x) \right| \leq \epsilon$ .

*Proof.* Apply Lemma 7 to  $f(x) = x/(1-x)$  on  $[0, \delta]$ . Following de Boor's equidistribution principle [De Boor, 1978], we select the adaptive grid nodes  $x_k = 1 - y_k^{-2}$  where  $y_k = 1 + \frac{k}{n}((1 -$

$\delta)^{-1/2} - 1$ ). Provided  $n \geq (1 - \delta)^{-1/2} - 1$ , we have  $y_k - y_{k-1} \leq 1$ , which strictly bounds the local error as  $\frac{1}{8}(x_k - x_{k-1})^2 \sup |f''(x)| \leq \frac{4}{n^2} ((1 - \delta)^{-1/2} - 1)^2$ . Enforcing  $\frac{4}{n^2} ((1 - \delta)^{-1/2} - 1)^2 \leq \epsilon$  yields the required condition  $n \geq 2((1 - \delta)^{-1/2} - 1) / \sqrt{\epsilon}$ .  $\square$

**Corollary 10** (Approximation of  $1/x$  on  $[\delta, 1]$ ). *Let  $\delta \in (0, 1)$  and target accuracy  $\epsilon \in (0, 1)$ . If the network width  $n \in \mathbb{N}$  satisfies*

$$n \geq 3/\sqrt{\delta\epsilon} = \mathcal{O}(1/\sqrt{\delta\epsilon}),$$

*then there exist parameters  $a_s, b_s, c_s \in \mathbb{R}$  for  $s \in [n]$ , and  $d \in \mathbb{R}$ , such that the neural network  $\phi(x) = \sum_{s=1}^n c_s \text{ReLU}(a_s x + b_s) + d$  satisfies  $\sup_{x \in [\delta, 1]} |1/x - \phi(x)| \leq \epsilon$ .*

*Proof.* Apply Lemma 7 to  $f(x) = 1/x$  on  $[\delta, 1]$ . Following de Boor’s equidistribution principle [De Boor, 1978], we select the adaptive grid nodes  $x_k = y_k^{-2}$  where  $y_k = \delta^{-1/2} - \frac{k}{n}(\delta^{-1/2} - 1)$ . Provided  $n \geq \delta^{-1/2} - 1$ , we have  $y_{k-1} - y_k \leq 1$ , which strictly bounds the local error as  $\frac{1}{8}(x_k - x_{k-1})^2 \sup |f''(x)| < \frac{9}{\delta n^2}$ . Enforcing  $\frac{9}{\delta n^2} \leq \epsilon$  yields the required condition  $n \geq 3/\sqrt{\delta\epsilon}$ .  $\square$

## C Construction of Transformers

### C.1 Overview of the Construction

We provide an overview of the transformer construction designed to implement the inexact preconditioned Richardson iteration. The construction includes three phases: read-in phase, iteration phase and read-out phase, where their detailed construction can be found in Appendices C.2, C.3, and C.4, respectively.

**Read-in Phase.** This phase serves as a preparatory step for the subsequent inexact Richardson iteration. Across three blocks, it approximates the preconditioner  $\mathbf{D}^{-1}$  and  $\mathbf{D}^{-1}\mathbf{y}$ :

- One transformer block approximates  $\alpha_i \approx \mathbf{D}_{ii}^{-1}$ . Specifically, its single-head attention layer exactly computes  $k_i \equiv 1/(1 + \sum_{j'=1}^N \mathcal{K}(\mathbf{x}_i, \mathbf{x}_{j'}))$ , and its MLP layer approximates  $\alpha_i \approx k_i/(1 - k_i) = \mathbf{D}_{ii}^{-1}$ .
- One MLP-only transformer block zeros out  $\alpha_{N+1}$ .
- One MLP-only transformer block approximates  $\beta_i \approx y_i \alpha_i$ .

**Iteration Phase.** The core optimization executes the iterative updates on  $\mathbf{w}$ :

- One transformer block exactly computes  $-\mathbf{D}^{-1}\mathbf{K}\mathbf{w}$ . Its single-head attention layer computes  $p_i \equiv -\mathbf{D}_{ii}^{-1} \sum_{j=1}^N \mathcal{K}(\mathbf{x}_i, \mathbf{x}_j) w_j$ , while its MLP layer zeros out  $p_{N+1}$ .
- One MLP-only transformer block implements the one-step inexact iteration update

$$\mathbf{w}^{(\ell+1)} = \mathbf{w}^{(\ell)} + \eta \left( \mathbf{D}^{-1}\mathbf{y} - \mathbf{D}^{-1}(\mathbf{K} + \lambda\mathbf{I})\mathbf{w}^{(\ell)} \right) + \mathbf{e}^{(\ell)},$$

where  $\mathbf{e}^{(\ell)}$  is the approximation error vector. This block also clears the  $p_i$  coordinate to reset the cache for future iterations.

**Read-out Phase.** The final blocks extract the prediction for the test token:

- One transformer block computes the normalized prediction and its inverse scaling factor for the test token. Its single-head attention layer exactly computes  $\widehat{p}_{N+1} \equiv k_{N+1} \sum_{j=1}^N \mathcal{K}(\mathbf{x}_{N+1}, \mathbf{x}_j) w_j$ , and its MLP layer approximates  $\widehat{k}_{N+1} \approx 1/k_{N+1}$ .
- One MLP-only transformer block approximates the product  $\widehat{p}_{N+1} \widehat{k}_{N+1}$  and writes the result to the target coordinate as the approximation for the Bayes optimal prediction  $\sum_{j=1}^N w_j^* \mathcal{K}(\mathbf{x}_{N+1}, \mathbf{x}_j)$ .

As detailed across the three phases above, each token  $\mathbf{z}_i$  is explicitly augmented to track these intermediate coordinates, structured as follows

$$\mathbf{z}_i = [\mathbf{x}_i^\top, y_i, w_i, \|\mathbf{x}_i\|_2^2, k_i, \alpha_i, \beta_i, p_i \text{ (or } \widehat{p}_i), \widehat{k}_i, s_i, t_i, 1]^\top.$$

## C.2 Read-in Phase

**One transformer block approximates  $D^{-1}$ .** We first construct a single-head attention layer. Set  $\mathbf{W}_Q, \mathbf{W}_K, \mathbf{W}_V \in \mathbb{R}^{D \times D}$  such that

$$\mathbf{W}_Q \mathbf{z}_i = [\mathbf{x}_i/v; \|\mathbf{x}_i\|^2/v; -(1-s_i)/(2v); \mathbf{0}], \quad \mathbf{W}_K \mathbf{z}_j = [\mathbf{x}_j/v; -(1-s_j)/(2v); \|\mathbf{x}_j\|^2/v; \mathbf{0}], \quad \mathbf{W}_V \mathbf{z}_j = s_j \mathbf{e}_{d+4}.$$

Note that for  $i, j \in \mathbb{Z}_{N+2}$ ,

$$\langle \mathbf{W}_Q \mathbf{z}_i, \mathbf{W}_K \mathbf{z}_j \rangle = \begin{cases} -\frac{\|\mathbf{x}_i - \mathbf{x}_j\|^2}{2v^2}, & \text{if } i, j \in [N+1], \\ 0, & \text{if } i = 0 \text{ or } j = 0, \end{cases} \quad \mathbf{W}_V \mathbf{z}_j = \begin{cases} \mathbf{0}, & \text{if } j \in [N+1], \\ \mathbf{e}_{d+4}, & \text{if } j = 0. \end{cases}$$

We mask out the test token, i.e., setting mask matrix  $\mathbf{M} \in \mathbb{R}^{(N+2) \times (N+2)}$  to be

$$\mathbf{M}_{ij} = \begin{cases} -\infty, & \text{if } j = N+1, \\ 0, & \text{otherwise.} \end{cases}$$

It follows that for all  $i \in [N]$ ,

$$\begin{aligned} \tilde{\mathbf{z}}_i &= \mathbf{z}_i + \sum_{j=0}^{N+1} \frac{\exp(\langle \mathbf{W}_Q \mathbf{z}_i, \mathbf{W}_K \mathbf{z}_j \rangle + \mathbf{M}_{ij})}{\sum_{j'=0}^{N+1} \exp(\langle \mathbf{W}_Q \mathbf{z}_i, \mathbf{W}_K \mathbf{z}_{j'} \rangle + \mathbf{M}_{ij'})} \mathbf{W}_V \mathbf{z}_j \\ &= \mathbf{z}_i + \sum_{j=0}^N \frac{\exp(\langle \mathbf{W}_Q \mathbf{z}_i, \mathbf{W}_K \mathbf{z}_j \rangle)}{\sum_{j'=0}^N \exp(\langle \mathbf{W}_Q \mathbf{z}_i, \mathbf{W}_K \mathbf{z}_{j'} \rangle)} \mathbf{W}_V \mathbf{z}_j \\ &= \mathbf{z}_i + \frac{\exp(\langle \mathbf{W}_Q \mathbf{z}_i, \mathbf{W}_K \mathbf{z}_0 \rangle)}{\sum_{j'=0}^N \exp(\langle \mathbf{W}_Q \mathbf{z}_i, \mathbf{W}_K \mathbf{z}_{j'} \rangle)} \mathbf{W}_V \mathbf{z}_0 + \sum_{j=1}^N \frac{\exp(\langle \mathbf{W}_Q \mathbf{z}_i, \mathbf{W}_K \mathbf{z}_j \rangle)}{\sum_{j'=0}^N \exp(\langle \mathbf{W}_Q \mathbf{z}_i, \mathbf{W}_K \mathbf{z}_{j'} \rangle)} \mathbf{W}_V \mathbf{z}_j \\ &= \mathbf{z}_i + \frac{1}{1 + \sum_{j'=1}^N \mathcal{K}(\mathbf{x}_i, \mathbf{x}_{j'})} \mathbf{e}_{d+4} \end{aligned}$$

and when  $i = 0$ ,

$$\begin{aligned} \tilde{\mathbf{z}}_0 &= \mathbf{z}_0 + \sum_{j=0}^{N+1} \frac{\exp(\langle \mathbf{W}_Q \mathbf{z}_0, \mathbf{W}_K \mathbf{z}_j \rangle + \mathbf{M}_{0j})}{\sum_{j'=0}^{N+1} \exp(\langle \mathbf{W}_Q \mathbf{z}_0, \mathbf{W}_K \mathbf{z}_{j'} \rangle + \mathbf{M}_{0j'})} \mathbf{W}_V \mathbf{z}_j \\ &= \mathbf{z}_0 + \frac{1}{\sum_{j'=0}^N \exp(\langle \mathbf{W}_Q \mathbf{z}_0, \mathbf{W}_K \mathbf{z}_{j'} \rangle)} \mathbf{e}_{d+4} = \mathbf{z}_0 + \frac{1}{1+N} \mathbf{e}_{d+4} \end{aligned}$$

and when  $i = N + 1$ ,

$$\begin{aligned}\tilde{\mathbf{z}}_{N+1} &= \mathbf{z}_{N+1} + \sum_{j=0}^{N+1} \frac{\exp(\langle \mathbf{W}_Q \mathbf{z}_{N+1}, \mathbf{W}_K \mathbf{z}_j \rangle + M_{N+1,j})}{\sum_{j'=0}^{N+1} \exp(\langle \mathbf{W}_Q \mathbf{z}_{N+1}, \mathbf{W}_K \mathbf{z}_{j'} \rangle + M_{N+1,j'})} \mathbf{W}_V \mathbf{z}_j \\ &= \mathbf{z}_{N+1} + \frac{1}{\sum_{j'=0}^N \exp(\langle \mathbf{W}_Q \mathbf{z}_{N+1}, \mathbf{W}_K \mathbf{z}_{j'} \rangle)} \mathbf{e}_{d+4} = \mathbf{z}_{N+1} + \frac{1}{1 + \sum_{j'=1}^N \mathcal{K}(\mathbf{x}_{N+1}, \mathbf{x}_{j'})} \mathbf{e}_{d+4}\end{aligned}$$

Let

$$k_i := \begin{cases} \frac{1}{1+N}, & \text{if } i = 0, \\ \frac{1}{1 + \sum_{j'=1}^N \mathcal{K}(\mathbf{x}_i, \mathbf{x}_{j'})}, & \text{if } i \in [N+1]. \end{cases} \quad (16)$$

We remark that the value of  $k_0$  is not important in the later analysis, and hence we replace this value by  $*$ . Then, after this attention layer, we have output<sup>1</sup>

$$\begin{bmatrix} \mathbf{x}_0 & \mathbf{x}_1 & \mathbf{x}_2 & \dots & \mathbf{x}_N & \mathbf{x}_{N+1} \\ 0 & y_1 & y_2 & \dots & y_N & 0 \\ 0 & w_1 & w_2 & \dots & w_N & 0 \\ 0 & \|\mathbf{x}_1\|^2 & \|\mathbf{x}_2\|^2 & \dots & \|\mathbf{x}_N\|^2 & \|\mathbf{x}_{N+1}\|^2 \\ * & \boxed{k_1} & \boxed{k_2} & \dots & \boxed{k_N} & \boxed{k_{N+1}} \\ \mathbf{0}_4 & \mathbf{0}_4 & \mathbf{0}_4 & \dots & \mathbf{0}_4 & \mathbf{0}_4 \\ s_0 & s_1 & s_2 & \dots & s_N & s_{N+1} \\ t_0 & t_1 & t_2 & \dots & t_N & t_{N+1} \\ 1 & 1 & 1 & \dots & 1 & 1 \end{bmatrix}.$$

We next construct the MLP layer in this transformer block. Let  $\epsilon_{\text{flip}} \in (0, 1)$ . According to Corollary 9 with  $\delta = 1/(1 + N\kappa_{\min})$ , there exist  $a_s, b_s, c_s \in [n_{\text{flip}}]$  with  $n_{\text{flip}} = \mathcal{O}(\sqrt{N/\epsilon_{\text{flip}}})$  such that

$$\sup_{x \in [0, \frac{1}{1+N\kappa_{\min}}]} \left| \frac{x}{1-x} - \phi_{\text{flip}}(x) \right| < \frac{\epsilon_{\text{flip}}}{N} \quad (17)$$

where  $\phi_{\text{flip}}(x) := \sum_{s=1}^{n_{\text{flip}}} c_s \text{ReLU}(a_s x + b_s)$ . Set  $\mathbf{W}_{\text{in}} \in \mathbb{R}^{n_{\text{flip}} \times D}$  and  $\mathbf{W}_{\text{out}} \in \mathbb{R}^{D \times n_{\text{flip}}}$  such that

$$\mathbf{W}_{\text{in}} \mathbf{z}_i = \begin{bmatrix} a_1 k_i + b_1 \\ a_2 k_i + b_2 \\ \vdots \\ a_{n_{\text{flip}}} k_i + b_{n_{\text{flip}}} \end{bmatrix}, \quad [\mathbf{W}_{\text{out}}]_{j,:} = \begin{cases} [c_1, c_2, \dots, c_{n_{\text{flip}}}], & \text{if } j = d+5, \\ \mathbf{0}, & \text{otherwise.} \end{cases}$$

For all  $i \in \mathbb{Z}_{N+2}$ , let  $\alpha_i := \phi_{\text{flip}}(k_i)$ . We ignore the estimate for  $i = 0$  as this value is not essential. Therefore, after this MLP layer, we have output

$$\begin{bmatrix} \mathbf{x}_0 & \mathbf{x}_1 & \mathbf{x}_2 & \dots & \mathbf{x}_N & \mathbf{x}_{N+1} \\ 0 & y_1 & y_2 & \dots & y_N & 0 \\ 0 & w_1 & w_2 & \dots & w_N & 0 \\ 0 & \|\mathbf{x}_1\|^2 & \|\mathbf{x}_2\|^2 & \dots & \|\mathbf{x}_N\|^2 & \|\mathbf{x}_{N+1}\|^2 \\ * & k_1 & k_2 & \dots & k_N & k_{N+1} \\ * & \boxed{\alpha_1} & \boxed{\alpha_2} & \dots & \boxed{\alpha_N} & \boxed{\alpha_{N+1}} \\ \mathbf{0}_3 & \mathbf{0}_3 & \mathbf{0}_3 & \dots & \mathbf{0}_3 & \mathbf{0}_3 \\ s_0 & s_1 & s_2 & \dots & s_N & s_{N+1} \\ t_0 & t_1 & t_2 & \dots & t_N & t_{N+1} \\ 1 & 1 & 1 & \dots & 1 & 1 \end{bmatrix}.$$

<sup>1</sup>Here, the entries wrapped in a box indicate the values that have been updated compared to the input.

As a remark at the end of this block, we let

$$r_i := \alpha_i - \mathbf{D}_{ii}^{-1}, \quad i \in [N+1], \quad (18)$$

and since  $0 < k_i < \frac{1}{1+N\kappa_{\min}}$ , we obtain from (17) that

$$|r_i| = |\mathbf{D}_{ii}^{-1} - \alpha_i| = \left| \frac{k_i}{1-k_i} - \alpha_i \right| < \frac{\epsilon_{\text{flip}}}{N}. \quad (19)$$

**One MLP-only transformer block zeros out  $\alpha_{N+1}$ .** It follows from (19) and the triangle inequality that for all  $i \in [N+1]$ ,

$$|\alpha_i| < \frac{1}{\sum_{j'=1}^N \mathcal{K}(\mathbf{x}_i, \mathbf{x}_{j'})} + \frac{\epsilon_{\text{flip}}}{N} < \frac{1}{N\kappa_{\min}} + \frac{1}{N} \equiv B_\alpha \quad (20)$$

Then we set  $\mathbf{W}_{\text{in}} \in \mathbb{R}^{2 \times D}$  and  $\mathbf{W}_{\text{out}} \in \mathbb{R}^{D \times 2}$  such that

$$\mathbf{W}_{\text{in}} \mathbf{z}_i = \begin{bmatrix} -\alpha_i - B_\alpha(1-t_i) \\ \alpha_i - B_\alpha(1-t_i) \end{bmatrix}, \quad [\mathbf{W}_{\text{out}}]_{j,:} = \begin{cases} [1, -1], & \text{if } j = d+5, \\ \mathbf{0}, & \text{otherwise.} \end{cases}$$

Recalling the definition of  $t_i$ , when  $i \in [N]$ , we have  $t_i = 0$ , and hence

$$\mathbf{z}_i + \mathbf{W}_{\text{out}} \text{ReLU}(\mathbf{W}_{\text{in}} \mathbf{z}_i) = \mathbf{z}_i + \text{ReLU}(-\alpha_i - B_\alpha) \mathbf{e}_{d+5} - \text{ReLU}(\alpha_i - B_\alpha) \mathbf{e}_{d+5} = \mathbf{z}_i;$$

moreover, when  $i = N+1$ , we have  $t_{N+1} = 1$ , which leads to

$$\mathbf{z}_{N+1} + \mathbf{W}_{\text{out}} \text{ReLU}(\mathbf{W}_{\text{in}} \mathbf{z}_{N+1}) = \mathbf{z}_{N+1} + \text{ReLU}(-\alpha_{N+1}) \mathbf{e}_{d+5} - \text{ReLU}(\alpha_{N+1}) \mathbf{e}_{d+5} = \mathbf{z}_{N+1} - \alpha_{N+1} \mathbf{e}_{d+5}.$$

So, after this MLP layer, we have output

$$\begin{bmatrix} \mathbf{x}_0 & \mathbf{x}_1 & \mathbf{x}_2 & \dots & \mathbf{x}_N & \mathbf{x}_{N+1} \\ 0 & y_1 & y_2 & \dots & y_N & 0 \\ 0 & w_1 & w_2 & \dots & w_N & 0 \\ 0 & \|\mathbf{x}_1\|^2 & \|\mathbf{x}_2\|^2 & \dots & \|\mathbf{x}_N\|^2 & \|\mathbf{x}_{N+1}\|^2 \\ * & k_1 & k_2 & \dots & k_N & k_{N+1} \\ * & \alpha_1 & \alpha_2 & \dots & \alpha_N & \boxed{0} \\ \mathbf{0}_3 & \mathbf{0}_3 & \mathbf{0}_3 & \dots & \mathbf{0}_3 & \mathbf{0}_3 \\ s_0 & s_1 & s_2 & \dots & s_N & s_{N+1} \\ t_0 & t_1 & t_2 & \dots & t_N & t_{N+1} \\ 1 & 1 & 1 & \dots & 1 & 1 \end{bmatrix}.$$

**One MLP-only transformer block approximates  $y_i \alpha_i$ .** Let  $\epsilon_{\text{sq}} \in (0, 1)$ . According to Corollary 8 with  $\delta = B_y + B_\alpha$ , there exist  $a_s, b_s, c_s \in [n_{\text{sq}}]$  with  $n_{\text{sq}} = \frac{B_y + B_\alpha}{\sqrt{\frac{\epsilon_{\text{sq}}}{N}}} = \mathcal{O}\left(\sqrt{\frac{N}{\epsilon_{\text{sq}}}}\right)$ , such that

$$\sup_{|x| \leq B_y + B_\alpha} |x^2 - \phi_{\text{sq}}(x)| < \frac{\epsilon_{\text{sq}}}{N}, \quad (21)$$

where  $\phi_{\text{sq}}(x) := \sum_{s=1}^{n_{\text{sq}}} c_s \text{ReLU}(a_s x + b_s)$ . We set  $\mathbf{W}_{\text{in}} \in \mathbb{R}^{2n_{\text{sq}} \times D}$  and  $\mathbf{W}_{\text{out}} \in \mathbb{R}^{D \times 2n_{\text{sq}}}$  such that

$$\mathbf{W}_{\text{in}} \mathbf{z}_i = \begin{bmatrix} a_1(y_i + \alpha_i) + b_1 \\ \vdots \\ a_{n_{\text{sq}}}(y_i + \alpha_i) + b_{n_{\text{sq}}} \\ a_1(y_i - \alpha_i) + b_1 \\ \vdots \\ a_{n_{\text{sq}}}(y_i - \alpha_i) + b_{n_{\text{sq}}} \end{bmatrix}, \quad [\mathbf{W}_{\text{out}}]_{j,:} = \begin{cases} \frac{\eta}{4}[c_1, \dots, c_{n_{\text{sq}}}, -c_1, \dots, -c_{n_{\text{sq}}}], & \text{if } j = d+6, \\ \mathbf{0}, & \text{otherwise.} \end{cases}$$

It turns out that for  $i \in \mathbb{Z}_{N+2}$ ,

$$\begin{aligned}\beta_i \equiv [\mathbf{W}_{\text{out}} \text{ReLU}(\mathbf{W}_{\text{in}} \mathbf{Z})]_{d+6,i} &= \frac{\eta}{4} \sum_{s=1}^{n_{\text{sq}}} c_s \text{ReLU}(a_s(y_i + \alpha_i) + b_s) - \frac{\eta}{4} \sum_{s=1}^{n_{\text{sq}}} c_s \text{ReLU}(a_s(y_i - \alpha_i) + b_s) \\ &= \frac{\eta}{4} (\phi_{\text{sq}}(y_i + \alpha_i) - \phi_{\text{sq}}(y_i - \alpha_i)).\end{aligned}$$

Since  $y_{N+1} = 0$  and  $\alpha_{N+1} = 0$ , we have  $\beta_{N+1} = \frac{\eta}{4} (\phi_{\text{sq}}(0) - \phi_{\text{sq}}(0)) = 0$ . So, after this MLP layer, we have output

$$\begin{bmatrix} \mathbf{x}_0 & \mathbf{x}_1 & \mathbf{x}_2 & \dots & \mathbf{x}_N & \mathbf{x}_{N+1} \\ 0 & y_1 & y_2 & \dots & y_N & 0 \\ 0 & w_1 & w_2 & \dots & w_N & 0 \\ 0 & \|\mathbf{x}_1\|^2 & \|\mathbf{x}_2\|^2 & \dots & \|\mathbf{x}_N\|^2 & \|\mathbf{x}_{N+1}\|^2 \\ * & k_1 & k_2 & \dots & k_N & k_{N+1} \\ * & \alpha_1 & \alpha_2 & \dots & \alpha_N & 0 \\ * & \boxed{\beta_1} & \boxed{\beta_2} & \dots & \boxed{\beta_N} & \boxed{0} \\ \mathbf{0}_2 & \mathbf{0}_2 & \mathbf{0}_2 & \dots & \mathbf{0}_2 & \mathbf{0}_2 \\ s_0 & s_1 & s_2 & \dots & s_N & s_{N+1} \\ t_0 & t_1 & t_2 & \dots & t_N & t_{N+1} \\ 1 & 1 & 1 & \dots & 1 & 1 \end{bmatrix}.$$

Moreover, when  $i \in [N]$ , let

$$\tau_{+,i} := \phi_{\text{sq}}(y_i + \alpha_i) - (y_i + \alpha_i)^2, \quad \tau_{-,i} := \phi_{\text{sq}}(y_i - \alpha_i) - (y_i - \alpha_i)^2.$$

Then we can rewrite  $\beta_i$  as

$$\beta_i = \frac{\eta}{4} ((y_i + \alpha_i)^2 + \tau_{+,i} - (y_i - \alpha_i)^2 - \tau_{-,i}) = \eta y_i \alpha_i + \frac{\eta}{4} (\tau_{+,i} - \tau_{-,i}). \quad (22)$$

Noting that  $|y_i \pm \alpha_i| \leq |y_i| + |\alpha_i| \leq B_y + B_\alpha$ , and by (21), we have

$$|\tau_{+,i}| \leq \frac{\epsilon_{\text{sq}}}{N}, \quad |\tau_{-,i}| \leq \frac{\epsilon_{\text{sq}}}{N}. \quad (23)$$

### C.3 Iteration Phase

**One transformer block exactly computes  $-D^{-1} \mathbf{K} \mathbf{w}$  and zeros out the corresponding feature for the test token.** We first construct a single-head attention layer. Set  $\sigma$  to be Softmax, and  $H = 1$ . Set  $\mathbf{W}_Q$ ,  $\mathbf{W}_K$  and  $\mathbf{W}_V$  such that

$$\mathbf{W}_Q \mathbf{z}_i = \frac{1}{v} [\mathbf{x}_i; \|\mathbf{x}_i\|^2; -1/2; \mathbf{0}], \quad \mathbf{W}_K \mathbf{z}_j = \frac{1}{v} [\mathbf{x}_j; -1/2; \|\mathbf{x}_j\|^2; \mathbf{0}], \quad \mathbf{W}_V \mathbf{z}_j = -w_j \mathbf{e}_{d+6}$$

Note that  $\langle \mathbf{W}_Q \mathbf{z}_i, \mathbf{W}_K \mathbf{z}_j \rangle = -\frac{\|\mathbf{x}_i - \mathbf{x}_j\|^2}{2v^2}$  for  $i, j \in \mathbb{Z}_{N+2}$ . We mask out the dummy token and the test token, i.e., setting mask matrix  $\mathbf{M} \in \mathbb{R}^{(N+2) \times (N+2)}$  to be

$$\mathbf{M}_{ij} = \begin{cases} -\infty, & \text{if } j = 0 \text{ or } j = N + 1, \\ 0, & \text{otherwise.} \end{cases}$$

It follows that for all  $i \in \mathbb{Z}_{N+2}$ ,

$$\sum_{j=0}^{N+1} \frac{\exp(\langle \mathbf{W}_Q \mathbf{z}_i, \mathbf{W}_K \mathbf{z}_j \rangle + \mathbf{M}_{ij})}{\sum_{j'=0}^{N+1} \exp(\langle \mathbf{W}_Q \mathbf{z}_i, \mathbf{W}_K \mathbf{z}_{j'} \rangle + \mathbf{M}_{ij'})} \mathbf{W}_V \mathbf{z}_j = - \sum_{j=1}^N \frac{\exp\left(-\frac{\|\mathbf{x}_i - \mathbf{x}_j\|^2}{2v^2}\right) w_j}{\sum_{j'=1}^N \exp\left(-\frac{\|\mathbf{x}_i - \mathbf{x}_{j'}\|^2}{2v^2}\right)} \mathbf{e}_{d+6} = p_i \mathbf{e}_{d+6}$$

where we denote

$$p_i := - \sum_{j=1}^N \frac{\mathcal{K}(\mathbf{x}_i, \mathbf{x}_j) w_j}{\sum_{j'=1}^N \mathcal{K}(\mathbf{x}_i, \mathbf{x}_{j'})}. \quad (24)$$

Again, the value of  $p_0$  is not important, hence we will hide it as  $*$ . So, after this attention layer, we have output

$$\begin{bmatrix} \mathbf{x}_0 & \mathbf{x}_1 & \mathbf{x}_2 & \dots & \mathbf{x}_N & \mathbf{x}_{N+1} \\ 0 & y_1 & y_2 & \dots & y_N & 0 \\ 0 & w_1 & w_2 & \dots & w_N & 0 \\ 0 & \|\mathbf{x}_1\|^2 & \|\mathbf{x}_2\|^2 & \dots & \|\mathbf{x}_N\|^2 & \|\mathbf{x}_{N+1}\|^2 \\ * & k_1 & k_2 & \dots & k_N & k_{N+1} \\ * & \alpha_1 & \alpha_2 & \dots & \alpha_N & 0 \\ * & \beta_1 & \beta_2 & \dots & \beta_N & 0 \\ \boxed{*} & \boxed{p_1} & \boxed{p_2} & \dots & \boxed{p_N} & \boxed{p_{N+1}} \\ 0 & 0 & 0 & \dots & 0 & 0 \\ s_0 & s_1 & s_2 & \dots & s_N & s_{N+1} \\ t_0 & t_1 & t_2 & \dots & t_N & t_{N+1} \\ 1 & 1 & 1 & \dots & 1 & 1 \end{bmatrix}.$$

We next construct an MLP layer to explicitly zero out  $p_{N+1}$ . Even if  $p_{N+1}$  is currently zero due to the initialization of the weights  $w_i = 0$ , it may become non-zero in later iterations. As we will see in the construction of the next block, the network executes the inexact preconditioned Richardson iteration (5), which updates the weights  $w_i$  for  $i \in [N]$ . Therefore, we would still need this layer to enforce  $p_{N+1} = 0$  across all iterations. By Theorem 5, we know that  $|w_j|$  for  $j \in [N]$  is bounded above by  $B_w$  during iterations, which guarantees that  $|p_i|$  is also bounded by  $B_w$ . That is,

$$|p_i| = \left| - \sum_{j=1}^N \frac{\mathcal{K}(\mathbf{x}_i, \mathbf{x}_j) w_j}{\sum_{j'=1}^N \mathcal{K}(\mathbf{x}_i, \mathbf{x}_{j'})} \right| \leq \max_{j \in [N]} |w_j| \leq B_w, \quad \forall i \in [N+1].$$

Then we set  $\mathbf{W}_{\text{in}} \in \mathbb{R}^{2 \times D}$  and  $\mathbf{W}_{\text{out}} \in \mathbb{R}^{D \times 2}$  such that

$$\mathbf{W}_{\text{in}} \mathbf{z}_i = \begin{bmatrix} -p_i - B_w(1 - t_i) \\ p_i - B_w(1 - t_i) \end{bmatrix}, \quad [\mathbf{W}_{\text{out}}]_{j,:} = \begin{cases} [1, -1], & \text{if } j = d+7, \\ \mathbf{0}, & \text{otherwise.} \end{cases}$$

Recalling the definition of  $t_i$ , when  $i \in [N]$ ,  $t_i = 0$ , and hence

$$\mathbf{z}_i + \mathbf{W}_{\text{out}} \text{ReLU}(\mathbf{W}_{\text{in}} \mathbf{z}_i) = \mathbf{z}_i + \text{ReLU}(-p_i - B_w) \mathbf{e}_{d+7} - \text{ReLU}(p_i - B_w) \mathbf{e}_{d+7} = \mathbf{z}_i,$$

moreover, when  $i = N+1$ ,  $t_{N+1} = 1$  gives

$$\mathbf{z}_{N+1} + \mathbf{W}_{\text{out}} \text{ReLU}(\mathbf{W}_{\text{in}} \mathbf{z}_{N+1}) = \mathbf{z}_{N+1} + \text{ReLU}(-p_{N+1}) \mathbf{e}_{d+7} - \text{ReLU}(p_{N+1}) \mathbf{e}_{d+7} = \mathbf{z}_{N+1} - p_{N+1} \mathbf{e}_{d+7}.$$

So, after this MLP layer, we have output

$$\begin{bmatrix} \mathbf{x}_0 & \mathbf{x}_1 & \mathbf{x}_2 & \dots & \mathbf{x}_N & \mathbf{x}_{N+1} \\ 0 & y_1 & y_2 & \dots & y_N & 0 \\ 0 & w_1 & w_2 & \dots & w_N & 0 \\ 0 & \|\mathbf{x}_1\|^2 & \|\mathbf{x}_2\|^2 & \dots & \|\mathbf{x}_N\|^2 & \|\mathbf{x}_{N+1}\|^2 \\ * & k_1 & k_2 & \dots & k_N & k_{N+1} \\ * & \alpha_1 & \alpha_2 & \dots & \alpha_N & 0 \\ * & \beta_1 & \beta_2 & \dots & \beta_N & 0 \\ * & p_1 & p_2 & \dots & p_N & \boxed{0} \\ 0 & 0 & 0 & \dots & 0 & 0 \\ s_0 & s_1 & s_2 & \dots & s_N & s_{N+1} \\ t_0 & t_1 & t_2 & \dots & t_N & t_{N+1} \\ 1 & 1 & 1 & \dots & 1 & 1 \end{bmatrix}.$$

**An MLP-only transformer block implements one-step inexact precondition Richardson update.** Let  $\tilde{\epsilon}_{\text{sq}} \in (0, 1)$ . According to Corollary 8 with  $\delta = B_w + B_\alpha$ , there exist

$$\tilde{n}_{\text{sq}} = \frac{B_w + B_\alpha}{\sqrt{\frac{\tilde{\epsilon}_{\text{sq}}}{N^2}}} = \mathcal{O}\left(\frac{\frac{1}{\sqrt{N}} + \frac{1}{N}}{\sqrt{\frac{\tilde{\epsilon}_{\text{sq}}}{N^2}}}\right) = \mathcal{O}\left(\sqrt{\frac{N}{\tilde{\epsilon}_{\text{sq}}}}\right),$$

such that

$$\sup_{|x| \leq B_w + B_\alpha} |x^2 - \tilde{\phi}_{\text{sq}}(x)| < \frac{\tilde{\epsilon}_{\text{sq}}}{N^2}, \quad (25)$$

where  $\tilde{\phi}_{\text{sq}}(x) := \sum_{s=1}^{\tilde{n}_{\text{sq}}} \tilde{c}_s \text{ReLU}(\tilde{a}_s x + \tilde{b}_s)$ . Set  $\mathbf{W}_{\text{in}} \in \mathbb{R}^{(2\tilde{n}_{\text{sq}}+4) \times D}$  such that

$$\mathbf{W}_{\text{in}} \mathbf{z}_i = \begin{bmatrix} \tilde{a}_1 (w_i + \alpha_i) + \tilde{b}_1 \\ \vdots \\ \tilde{a}_{\tilde{n}_{\text{sq}}} (w_i + \alpha_i) + \tilde{b}_{\tilde{n}_{\text{sq}}} \\ \tilde{a}_1 (w_i - \alpha_i) + \tilde{b}_1 \\ \vdots \\ \tilde{a}_{\tilde{n}_{\text{sq}}} (w_i - \alpha_i) + \tilde{b}_{\tilde{n}_{\text{sq}}} \\ \beta_i \\ -\beta_i \\ p_i \\ -p_i \end{bmatrix}$$

and set  $\mathbf{W}_{\text{out}} \in \mathbb{R}^{D \times (2\tilde{n}_{\text{sq}}+4)}$  such that

$$[\mathbf{W}_{\text{out}}]_{j,:} = \begin{cases} \left[ -\frac{\eta \lambda \tilde{c}_1}{4}, \dots, -\frac{\eta \lambda \tilde{c}_{\tilde{n}_{\text{sq}}}}{4}, \frac{\eta \lambda \tilde{c}_1}{4}, \dots, \frac{\eta \lambda \tilde{c}_{\tilde{n}_{\text{sq}}}}{4}, 1, -1, \eta, -\eta \right], & \text{if } j = d + 2, \\ [0, 0, \dots, 0, -1, 1], & \text{if } j = d + 7, \\ \mathbf{0}, & \text{otherwise.} \end{cases}$$

It turns out that for  $i \in \mathbb{Z}_{N+2}$ ,

$$\begin{aligned}
& [\mathbf{W}_{\text{out}}\text{ReLU}(\mathbf{W}_{\text{in}}\mathbf{Z})]_{d+2,i} \\
&= -\frac{\eta\lambda}{4} \left( \sum_{s=1}^{\tilde{n}_{\text{sq}}} \tilde{c}_s \text{ReLU}(\tilde{a}_s(w_i + \alpha_i) + \tilde{b}_s) - \sum_{s=1}^{\tilde{n}_{\text{sq}}} \tilde{c}_s \text{ReLU}(\tilde{a}_s(w_i - \alpha_i) + \tilde{b}_s) \right) \\
&\quad + (\text{ReLU}(\beta_i) - \text{ReLU}(-\beta_i)) + \eta(\text{ReLU}(p_i) - \text{ReLU}(-p_i)) \\
&= -\frac{\eta\lambda}{4} \left( \tilde{\phi}_{\text{sq}}(w_i + \alpha_i) - \tilde{\phi}_{\text{sq}}(w_i - \alpha_i) \right) + \beta_i + \eta p_i
\end{aligned} \tag{26}$$

and

$$[\mathbf{W}_{\text{out}}\text{ReLU}(\mathbf{W}_{\text{in}}\mathbf{Z})]_{d+6,i} = -\text{ReLU}(p_i) + \text{ReLU}(-p_i) = -p_i.$$

We first look at the update at the  $(d+2)$ -th row.

- When  $i = N+1$ , note that  $\beta_{N+1} = 0$ ,  $w_{N+1} = 0$ ,  $\alpha_{N+1} = 0$  and  $p_{N+1} = 0$ . Hence (26) with  $i = N+1$  gives

$$\Delta w_{N+1} \equiv [\mathbf{W}_{\text{out}}\text{ReLU}(\mathbf{W}_{\text{in}}\mathbf{Z})]_{d+2,N+1} = -\frac{\eta\lambda}{4} \left( \tilde{\phi}_{\text{sq}}(0) - \tilde{\phi}_{\text{sq}}(0) \right) = 0.$$

- Now we consider  $i \in [N]$ . Let

$$\tilde{\tau}_{+,i} := \tilde{\phi}_{\text{sq}}(w_i + \alpha_i) - (w_i + \alpha_i)^2, \quad \tilde{\tau}_{-,i} := \tilde{\phi}_{\text{sq}}(w_i - \alpha_i) - (w_i - \alpha_i)^2.$$

Note that  $|w_i \pm \alpha_i| \leq |w_i| + |\alpha_i| \leq B_w + B_\alpha$ , which with (25) implies

$$|\tilde{\tau}_{+,i}| \leq \frac{\tilde{\epsilon}_{\text{sq}}}{N^2}, \quad |\tilde{\tau}_{-,i}| \leq \frac{\tilde{\epsilon}_{\text{sq}}}{N^2}. \tag{27}$$

Then with the above notations and using forms (18), (22), (24) for  $r_i$ ,  $\beta_i$  and  $p_i$ , we proceed from (26) to obtain that for  $i \in [N]$ ,

$$\begin{aligned}
\Delta w_i &\equiv [\mathbf{W}_{\text{out}}\text{ReLU}(\mathbf{W}_{\text{in}}\mathbf{Z})]_{d+2,i} \\
&= -\frac{\eta\lambda}{4} \left( (w_i + \alpha_i)^2 + \tilde{\tau}_{+,i} - (w_i - \alpha_i)^2 - \tilde{\tau}_{-,i} \right) + \beta_i + \eta p_i \\
&= \eta(y_i - \lambda w_i)\alpha_i + \eta p_i + \frac{\eta}{4}(\tau_{+,i} - \tau_{-,i}) - \frac{\eta\lambda}{4}(\tilde{\tau}_{+,i} - \tilde{\tau}_{-,i}) \\
&= \eta(y_i - \lambda w_i)\mathbf{D}_{ii}^{-1} - \eta\mathbf{D}_{ii}^{-1} \sum_{j=1}^N \mathcal{K}(\mathbf{x}_i, \mathbf{x}_j)w_j + \frac{\eta}{4}(\tau_{+,i} - \tau_{-,i}) - \frac{\eta\lambda}{4}(\tilde{\tau}_{+,i} - \tilde{\tau}_{-,i}) + \eta(y_i - \lambda w_i)r_i
\end{aligned}$$

Therefore, with the residual connection, we have updated at the  $(d+2)$ -th row

$$w_i \leftarrow w_i + \Delta w_i.$$

Moreover, the update at the  $(d+6)$ -th row is

$$p_i \leftarrow p_i - p_i = 0.$$

After this MLP layer, we have output

$$\begin{bmatrix} \mathbf{x}_0 & \mathbf{x}_1 & \mathbf{x}_2 & \dots & \mathbf{x}_N & \mathbf{x}_{N+1} \\ 0 & y_1 & y_2 & \dots & y_N & 0 \\ * & w_1 + \Delta w_1 & w_2 + \Delta w_2 & \dots & w_N + \Delta w_N & 0 \\ 0 & \|\mathbf{x}_1\|^2 & \|\mathbf{x}_2\|^2 & \dots & \|\mathbf{x}_N\|^2 & \|\mathbf{x}_{N+1}\|^2 \\ * & k_1 & k_2 & \dots & k_N & k_{N+1} \\ * & \alpha_1 & \alpha_2 & \dots & \alpha_N & 0 \\ * & \beta_1 & \beta_2 & \dots & \beta_N & 0 \\ 0 & 0 & 0 & \dots & 0 & 0 \\ 0 & 0 & 0 & \dots & 0 & 0 \\ s_0 & s_1 & s_2 & \dots & s_N & s_{N+1} \\ t_0 & t_1 & t_2 & \dots & t_N & t_{N+1} \\ 1 & 1 & 1 & \dots & 1 & 1 \end{bmatrix}$$

We notice that the constructed transformer implements the following update

$$w_i \leftarrow w_i + \eta \left( (y_i - \lambda w_i) \mathbf{D}_{ii}^{-1} - \mathbf{D}_{ii}^{-1} \sum_{j=1}^N \mathcal{K}(\mathbf{x}_i, \mathbf{x}_j) w_j \right) + \eta \left( (y_i - \lambda w_i) r_i + \frac{\tau_{+,i} - \tau_{-,i} - \lambda \tilde{\tau}_{+,i} + \lambda \tilde{\tau}_{-,i}}{4} \right).$$

In vector form, it is the inexact preconditioned Richardson iteration (5) with

$$\begin{aligned} \mathbf{r} &:= [r_i : i \in [N]], \quad \boldsymbol{\tau}_+ := [\tau_{+,i} : i \in [N]], \quad \boldsymbol{\tau}_- := [\tau_{-,i} : i \in [N]] \\ \tilde{\boldsymbol{\tau}}_+^{(\ell)} &:= [\tilde{\tau}_{+,i}^{(\ell)} : i \in [N]], \quad \tilde{\boldsymbol{\tau}}_-^{(\ell)} := [\tilde{\tau}_{-,i}^{(\ell)} : i \in [N]], \end{aligned}$$

satisfying (6), due to properties (19), (23) and (27) guaranteed in the construction. Here, the error vectors  $\boldsymbol{\tau}$ ,  $\boldsymbol{\tau}_+$ , and  $\boldsymbol{\tau}_-$  do not depend on  $\mathbf{w}^{(\ell)}$  and therefore remain unchanged throughout the iterations. On the other hand,  $\tilde{\boldsymbol{\tau}}_+^{(\ell)}$  and  $\tilde{\boldsymbol{\tau}}_-^{(\ell)}$  do depend on  $\mathbf{w}^{(\ell)}$ , which is the reason why they carry the index  $\ell$ .

We remark that the two blocks constructed in this phase implement a single step of the inexact preconditioned Richardson iteration. By sequentially repeating this construction, the transformer effectively executes multiple iterations of the algorithm.

#### C.4 Read-out Phase

**One transformer block computes the test token's normalized prediction and inverse scaling factor.** We first construct a single-head attention layer. Set  $\mathbf{W}_Q$ ,  $\mathbf{W}_K$  and  $\mathbf{W}_V$  such that

$$\mathbf{W}_Q \mathbf{z}_i = \frac{1}{v} [\mathbf{x}_i; \|\mathbf{x}_i\|^2; -1/2; \mathbf{0}], \quad \mathbf{W}_K \mathbf{z}_j = \frac{1}{v} [\mathbf{x}_j; -1/2; \|\mathbf{x}_j\|^2; \mathbf{0}], \quad \mathbf{W}_V \mathbf{z}_j = w_j \mathbf{e}_{d+7}.$$

Note that  $\langle \mathbf{W}_Q \mathbf{z}_i, \mathbf{W}_K \mathbf{z}_j \rangle = -\frac{\|\mathbf{x}_i - \mathbf{x}_j\|^2}{2v^2}$ . We mask out the dummy token, i.e., setting mask matrix  $\mathbf{M} \in \mathbb{R}^{(N+2) \times (N+2)}$  to be

$$\mathbf{M}_{ij} = \begin{cases} -\infty, & \text{if } j = 0, \\ 0, & \text{otherwise.} \end{cases}$$

It follows that for all  $i \in [N + 1]$ ,

$$\begin{aligned} & \sum_{j=0}^{N+1} \frac{\exp(\langle \mathbf{W}_Q \mathbf{z}_i, \mathbf{W}_K \mathbf{z}_j \rangle + \mathbf{M}_{ij})}{\sum_{j'=0}^{N+1} \exp(\langle \mathbf{W}_Q \mathbf{z}_i, \mathbf{W}_K \mathbf{z}_{j'} \rangle + \mathbf{M}_{ij'})} \mathbf{W}_V \mathbf{z}_j = \sum_{j=1}^{N+1} \frac{\exp\left(-\frac{\|\mathbf{x}_i - \mathbf{x}_j\|^2}{2v^2}\right) w_j}{\sum_{j'=1}^{N+1} \exp\left(-\frac{\|\mathbf{x}_i - \mathbf{x}_{j'}\|^2}{2v^2}\right)} \mathbf{e}_{d+7} \\ & = \sum_{j=1}^{N+1} \frac{\mathcal{K}(\mathbf{x}_i, \mathbf{x}_j) w_j}{\sum_{j'=1}^{N+1} \mathcal{K}(\mathbf{x}_i, \mathbf{x}_{j'})} \mathbf{e}_{d+7} = \underbrace{\sum_{j=1}^N \frac{\mathcal{K}(\mathbf{x}_i, \mathbf{x}_j) w_j}{\sum_{j'=1}^{N+1} \mathcal{K}(\mathbf{x}_i, \mathbf{x}_{j'})}}_{\text{denoted by } \hat{p}_i} \mathbf{e}_{d+7} \end{aligned}$$

where the last equality uses  $w_{N+1} = 0$ . In particular, when  $i = N + 1$ , the value is

$$\begin{aligned} \hat{p}_{N+1} & = \sum_{j=1}^N \frac{\mathcal{K}(\mathbf{x}_{N+1}, \mathbf{x}_j) w_j}{\sum_{j'=1}^{N+1} \mathcal{K}(\mathbf{x}_{N+1}, \mathbf{x}_{j'})} = \frac{1}{1 + \sum_{j'=1}^N \mathcal{K}(\mathbf{x}_{N+1}, \mathbf{x}_{j'})} \sum_{j=1}^N \mathcal{K}(\mathbf{x}_{N+1}, \mathbf{x}_j) w_j \\ & = k_{N+1} \sum_{j=1}^N \mathcal{K}(\mathbf{x}_{N+1}, \mathbf{x}_j) w_j \end{aligned}$$

where the last equation follows from definition (16) of  $k_{N+1}$ . Note that the  $(d + 7)$ -th row of the input is a zero vector, and we only care about the feature  $\hat{p}_{N+1}$  for the test token (the features for the training tokens are hidden as  $*$ ). Therefore, after this attention layer, the output is

$$\begin{bmatrix} \mathbf{x}_0 & \mathbf{x}_1 & \mathbf{x}_2 & \dots & \mathbf{x}_N & \mathbf{x}_{N+1} \\ 0 & y_1 & y_2 & \dots & y_N & 0 \\ * & w_1 & w_2 & \dots & w_N & 0 \\ 0 & \|\mathbf{x}_1\|^2 & \|\mathbf{x}_2\|^2 & \dots & \|\mathbf{x}_N\|^2 & \|\mathbf{x}_{N+1}\|^2 \\ * & k_1 & k_2 & \dots & k_N & k_{N+1} \\ * & \alpha_1 & \alpha_2 & \dots & \alpha_N & 0 \\ * & \beta_1 & \beta_2 & \dots & \beta_N & 0 \\ \boxed{*} & \boxed{*} & \boxed{*} & \dots & \boxed{*} & \boxed{\hat{p}_{N+1}} \\ 0 & 0 & 0 & \dots & 0 & 0 \\ s_0 & s_1 & s_2 & \dots & s_N & s_{N+1} \\ t_0 & t_1 & t_2 & \dots & t_N & t_{N+1} \\ 1 & 1 & 1 & \dots & 1 & 1 \end{bmatrix}.$$

**One MLP-only transformer block approximates  $1/k_{N+1}$ .** Let  $\epsilon_{\text{inv}} \in (0, 1)$ . According to Corollary 10 with  $\delta = 1/(N + 1)$ , there exist  $a_s, b_s, c_s \in [n_{\text{inv}}]$  with  $n_{\text{inv}} = 3/\sqrt{\delta \epsilon_{\text{inv}}} = \mathcal{O}(\sqrt{N}/\epsilon_{\text{inv}})$ , such that

$$\sup_{x \in [\frac{1}{N+1}, 1]} \left| \frac{1}{x} - \phi_{\text{inv}}(x) \right| < \epsilon_{\text{inv}} \quad (28)$$

where  $\phi_{\text{inv}}(x) := \sum_{s=1}^{n_{\text{inv}}} c_s \text{ReLU}(a_s x + b_s)$ . Set  $\mathbf{W}_{\text{in}} \in \mathbb{R}^{n_{\text{inv}} \times D}$  and  $\mathbf{W}_{\text{out}} \in \mathbb{R}^{D \times n_{\text{inv}}}$  such that

$$\mathbf{W}_{\text{in}} \mathbf{z}_i = \begin{bmatrix} a_1 k_i + b_1 \\ a_2 k_i + b_2 \\ \vdots \\ a_{n_{\text{inv}}} k_i + b_{n_{\text{inv}}} \end{bmatrix}, \quad [\mathbf{W}_{\text{out}}]_{j,:} = \begin{cases} [c_1, c_2, \dots, c_{n_{\text{inv}}}], & \text{if } j = d + 8, \\ \mathbf{0}, & \text{otherwise.} \end{cases}$$

Let  $\widehat{k}_i := \phi_{\text{inv}}(k_i)$ . It turns out that for  $i \in \mathbb{Z}_{N+2}$ ,  $[\mathbf{W}_{\text{out}} \text{ReLU}(\mathbf{W}_{\text{in}} \mathbf{Z})]_{d+8,i} = \widehat{k}_i$ . In particular, we only need the case  $i = N + 1$ , and the output of this MLP layer is

$$\begin{bmatrix} \mathbf{x}_0 & \mathbf{x}_1 & \mathbf{x}_2 & \dots & \mathbf{x}_N & \mathbf{x}_{N+1} \\ 0 & y_1 & y_2 & \dots & y_N & 0 \\ * & w_1 & w_2 & \dots & w_N & 0 \\ 0 & \|\mathbf{x}_1\|^2 & \|\mathbf{x}_2\|^2 & \dots & \|\mathbf{x}_N\|^2 & \|\mathbf{x}_{N+1}\|^2 \\ * & k_1 & k_2 & \dots & k_N & k_{N+1} \\ * & \alpha_1 & \alpha_2 & \dots & \alpha_N & 0 \\ * & * & * & \dots & * & \widehat{p}_{N+1} \\ \boxed{*} & \boxed{*} & \boxed{*} & \dots & \boxed{*} & \boxed{\widehat{k}_{N+1}} \\ s_0 & s_1 & s_2 & \dots & s_N & s_{N+1} \\ t_0 & t_1 & t_2 & \dots & t_N & t_{N+1} \\ 1 & 1 & 1 & \dots & 1 & 1 \end{bmatrix}.$$

Moreover, we remark that

$$\frac{1}{1+N} \leq k_i = \frac{1}{1 + \sum_{j'=1}^N \mathcal{K}(\mathbf{x}_i, \mathbf{x}_{j'})} \leq 1, \quad \forall i \in [N+1].$$

The above estimate with (28) implies

$$\left| \frac{1}{k_i} - \widehat{k}_i \right| < \epsilon_{\text{inv}}. \quad (29)$$

**One MLP-only transformer block approximates the product  $\widehat{k}_{N+1} \widehat{p}_{N+1}$ .** Let  $\widehat{\epsilon}_{\text{sq}} \in (0, 1)$ . According to Corollary 8 with  $\delta = B_w + 3$ , there exist  $\widehat{a}_s, \widehat{b}_s, \widehat{c}_s \in [\widehat{n}_{\text{sq}}]$  with  $\widehat{n}_{\text{sq}} = \mathcal{O}(\sqrt{N/\widehat{\epsilon}_{\text{sq}}})$ , such that

$$\sup_{|x| \leq B_w + 3} \left| x^2 - \widehat{\phi}_{\text{sq}}(x) \right| < \frac{\widehat{\epsilon}_{\text{sq}}}{N}, \quad (30)$$

where  $\widehat{\phi}_{\text{sq}}(x) := \sum_{s=1}^{\widehat{n}_{\text{sq}}} \widehat{c}_s \text{ReLU}(\widehat{a}_s x + \widehat{b}_s)$ . Set  $\mathbf{W}_{\text{in}} \in \mathbb{R}^{2\widehat{n}_{\text{sq}} \times D}$  and  $\mathbf{W}_{\text{out}} \in \mathbb{R}^{D \times 2\widehat{n}_{\text{sq}}}$  such that

$$\mathbf{W}_{\text{in}} \mathbf{z}_i = \begin{bmatrix} \widehat{a}_1 \left( \widehat{k}_i/N + \widehat{p}_i \right) + \widehat{b}_1 \\ \widehat{a}_2 \left( \widehat{k}_i/N + \widehat{p}_i \right) + \widehat{b}_2 \\ \vdots \\ \widehat{a}_{\widehat{n}_{\text{sq}}} \left( \widehat{k}_i/N + \widehat{p}_i \right) + \widehat{b}_{\widehat{n}_{\text{sq}}} \\ \widehat{a}_1 \left( \widehat{k}_i/N - \widehat{p}_i \right) + \widehat{b}_1 \\ \widehat{a}_2 \left( \widehat{k}_i/N - \widehat{p}_i \right) + \widehat{b}_2 \\ \vdots \\ \widehat{a}_{\widehat{n}_{\text{sq}}} \left( \widehat{k}_i/N - \widehat{p}_i \right) + \widehat{b}_{\widehat{n}_{\text{sq}}} \end{bmatrix},$$

and

$$[\mathbf{W}_{\text{out}}]_{j,:} = \begin{cases} \frac{N}{4} [\widehat{c}_1, \widehat{c}_2, \dots, \widehat{c}_{\widehat{n}_{\text{sq}}}, -\widehat{c}_1, -\widehat{c}_2, \dots, -\widehat{c}_{\widehat{n}_{\text{sq}}}], & \text{if } j = d + 1, \\ \mathbf{0}, & \text{otherwise.} \end{cases}$$

Therefore, for  $i \in \mathbb{Z}_{N+2}$ ,

$$o_i := [\mathbf{W}_{\text{out}} \text{ReLU}(\mathbf{W}_{\text{in}} \mathbf{Z})]_{d+1, i} = \frac{N}{4} \left( \widehat{\phi}_{\text{sq}}(\widehat{k}_i/N + \widehat{p}_i) - \widehat{\phi}_{\text{sq}}(\widehat{k}_i/N - \widehat{p}_i) \right). \quad (31)$$

Thus, after this layer, we have output

$$\begin{bmatrix} \mathbf{x}_0 & \mathbf{x}_1 & \mathbf{x}_2 & \dots & \mathbf{x}_N & \mathbf{x}_{N+1} \\ \boxed{*} & \boxed{y_1 + * } & \boxed{y_2 + * } & \dots & \boxed{y_N + * } & \boxed{o_{N+1}} \\ * & w_1 & w_2 & \dots & w_N & 0 \\ 0 & \|\mathbf{x}_1\|^2 & \|\mathbf{x}_2\|^2 & \dots & \|\mathbf{x}_N\|^2 & \|\mathbf{x}_{N+1}\|^2 \\ * & k_1 & k_2 & \dots & k_N & k_{N+1} \\ * & \alpha_1 & \alpha_2 & \dots & \alpha_N & 0 \\ * & \beta_1 & \beta_2 & \dots & \beta_N & 0 \\ * & * & * & \dots & * & \widehat{p}_{N+1} \\ * & * & * & \dots & * & \widehat{k}_{N+1} \\ s_0 & s_1 & s_2 & \dots & s_N & s_{N+1} \\ t_0 & t_1 & t_2 & \dots & t_N & t_{N+1} \\ 1 & 1 & 1 & \dots & 1 & 1 \end{bmatrix}.$$

Moreover, when  $i \in [N+1]$ , let

$$\widehat{\tau}_{+,i} := \widehat{\phi}_{\text{sq}}(\widehat{k}_i/N + \widehat{p}_i) - (\widehat{k}_i/N + \widehat{p}_i)^2, \quad \widehat{\tau}_{-,i} := \widehat{\phi}_{\text{sq}}(\widehat{k}_i/N - \widehat{p}_i) - (\widehat{k}_i/N - \widehat{p}_i)^2.$$

It follows that  $o_i$  can be rewritten as

$$o_i = \frac{N}{4} \left( (\widehat{k}_i/N + \widehat{p}_i)^2 - (\widehat{k}_i/N - \widehat{p}_i)^2 + \widehat{\tau}_{+,i} - \widehat{\tau}_{-,i} \right) = \widehat{k}_i \widehat{p}_i + \frac{N}{4} (\widehat{\tau}_{+,i} - \widehat{\tau}_{-,i}). \quad (32)$$

Recall that  $|w_j|$ ,  $j \in [N]$  are bounded by  $B_w$ , hence  $\widehat{p}_i$  is also bounded by  $B_w$ . That is,

$$|\widehat{p}_i| = \left| \sum_{j=1}^N \frac{\mathcal{K}(\mathbf{x}_i, \mathbf{x}_j) w_j}{\sum_{j'=1}^{N+1} \mathcal{K}(\mathbf{x}_i, \mathbf{x}_{j'})} \right| \leq \max_{j \in [N]} |w_j| \leq B_w, \quad \forall i \in [N+1].$$

Furthermore, it follows from (29) that

$$\left| \frac{\widehat{k}_i}{N} \right| < \frac{1}{N} \left( \frac{1}{\widehat{k}_i} + \epsilon_{\text{inv}} \right) = \frac{1}{N} \left( 1 + \sum_{j=1}^N \mathcal{K}(\mathbf{x}_i, \mathbf{x}_j) + \epsilon_{\text{inv}} \right) < \frac{2+N}{N} \leq 3.$$

Therefore,  $\left| \frac{\widehat{k}_i}{N} \pm \widehat{p}_i \right| \leq \left| \frac{\widehat{k}_i}{N} \right| + |\widehat{p}_i| < 3 + B_w$ . Combining this with (30) implies

$$|\widehat{\tau}_{\pm, i}| < \widehat{\epsilon}_{\text{sq}}/N. \quad (33)$$

## C.5 Analysis

**Proposition 11.** *Suppose that assumptions of Theorem 5 hold and  $\mathbf{w}^* = [w_i^* : i \in [N]]$  is the solution of linear system (2). Let TF denote the complete transformer network constructed by composing the read-in blocks from Appendix C.2,  $\ell$  repetitions of the iteration blocks from Appendix C.3, and the read-out blocks from Appendix C.4. Then*

$$\begin{aligned} & \left| \text{readout}(\text{TF}(\mathbf{Z})) - \sum_{i=1}^N w_i^* \mathcal{K}(\mathbf{x}_i, \mathbf{x}_{N+1}) \right| \\ & \leq (1 - \eta \lambda_0 (1 - c))^\ell \frac{\left( \frac{1}{\sqrt{\lambda_0}} + 1 \right) B_y}{\lambda_0 \sqrt{\kappa_{\text{min}}}} + \frac{\frac{B_y}{\sqrt{\lambda_0}} \epsilon_{\text{flip}} + (1 + \lambda_0) (\epsilon_{\text{sq}} + \widetilde{\epsilon}_{\text{sq}})}{\lambda_0 (1 - c) \sqrt{\kappa_{\text{min}}}} + \frac{\widehat{\epsilon}_{\text{sq}}}{2} + \epsilon_{\text{inv}} \widetilde{B}_w, \end{aligned}$$

where

$$\tilde{B}_w := \frac{\left(\frac{1}{\sqrt{\lambda_0}} + 1\right) B_y}{\lambda_0 \sqrt{\kappa_{\min}}} + \frac{\frac{B_y}{\sqrt{\lambda_0}} + 2(1 + \lambda_0)}{\lambda_0(1-c)\sqrt{\kappa_{\min}}} + \frac{\left(\frac{1}{\sqrt{\lambda_0}} + 1\right) B_y}{\lambda_0}.$$

*Proof.* It follows from (32) and (33) with  $i = N + 1$  that

$$\left|o_{N+1} - \hat{k}_{N+1}\hat{p}_{N+1}\right| = \frac{N}{4} |\hat{\tau}_{+,i} - \hat{\tau}_{-,i}| \leq \frac{\hat{\epsilon}_{\text{sq}}}{2}. \quad (34)$$

Note that by definition of  $\hat{p}_{N+1}$  and relation (29), we have

$$\begin{aligned} & \left| \hat{k}_{N+1}\hat{p}_{N+1} - \sum_{j=1}^N \mathcal{K}(\mathbf{x}_{N+1}, \mathbf{x}_j) w_j^{(\ell)} \right| = \left| \hat{k}_{N+1}k_{N+1} - 1 \right| \left| \sum_{j=1}^N \mathcal{K}(\mathbf{x}_{N+1}, \mathbf{x}_j) w_j^{(\ell)} \right| \\ & < \epsilon_{\text{inv}} k_{N+1} \left| \sum_{j=1}^N \mathcal{K}(\mathbf{x}_{N+1}, \mathbf{x}_j) w_j^{(\ell)} \right| \leq \epsilon_{\text{inv}} \left| \sum_{j=1}^N \frac{\mathcal{K}(\mathbf{x}_{N+1}, \mathbf{x}_j)}{1 + \sum_{j=1}^N \mathcal{K}(\mathbf{x}_{N+1}, \mathbf{x}_j)} \right| \|\mathbf{w}^{(\ell)}\|_{\infty} \leq \epsilon_{\text{inv}} B_w \leq \epsilon_{\text{inv}} \tilde{B}_w, \end{aligned} \quad (35)$$

where in the last inequality, we relax the bound  $B_w$  to a strictly larger value  $\tilde{B}_w$  that is independent of  $N$ . Hence, by triangle inequality and estimates (34), (35), we obtain

$$\left| o_{N+1} - \sum_{j=1}^N \mathcal{K}(\mathbf{x}_{N+1}, \mathbf{x}_j) w_j^{(\ell)} \right| \leq \frac{\hat{\epsilon}_{\text{sq}}}{2} + \epsilon_{\text{inv}} \tilde{B}_w.$$

Combining this with Proposition 6 and triangle inequality gives the estimate of  $\left| o_{N+1} - \sum_{i=1}^N w_i^* \mathcal{K}(\mathbf{x}_i, \mathbf{x}_{N+1}) \right|$ . The desired result immediately follows by noting that

$$o_{N+1} = \text{readout}(\text{TF}).$$

□

**Theorem 12** (Formal version of Theorem 1). *Let  $\varepsilon \in (0, c)$  for a constant  $c \in (0, 1)$ . Let  $\lambda_0 > 0$  and  $\eta$  satisfy (11). There exists a single-head transformer network TF consisting of  $(2L + 5)$  blocks with MLP width  $W$  such that the final prediction satisfies*

$$\left| \text{readout}(\text{TF}(\mathbf{Z})) - \sum_{i=1}^N w_i^* \mathcal{K}(\mathbf{x}_i, \mathbf{x}_{N+1}) \right| \leq C_{\text{sys}} \varepsilon.$$

where the constant  $C_{\text{sys}}$  is defined by

$$C_{\text{sys}} := \frac{\left(\frac{1}{\sqrt{\lambda_0}} + 1\right) B_y}{\lambda_0} \left( \frac{2}{\sqrt{\kappa_{\min}}} + 1 \right) + 2 \frac{\frac{B_y}{\sqrt{\lambda_0}} + 2(1 + \lambda_0)}{\lambda_0(1-c)\sqrt{\kappa_{\min}}} + \frac{1}{2},$$

the iteration count  $L$  is

$$L := \left\lceil \frac{\log(1/\varepsilon)}{\log(1/(1 - \eta\lambda_0(1-c)))} \right\rceil = \mathcal{O}(\log(1/\varepsilon)), \quad (36)$$

the maximum MLP width is

$$W := \max \{n_{\text{flip}}, 2n_{\text{sq}}, 2\tilde{n}_{\text{sq}} + 4, n_{\text{inv}}, 2\hat{n}_{\text{sq}}, 2\} = \mathcal{O}(\sqrt{N/\varepsilon}),$$

in which

$$\begin{aligned} n_{\text{flip}} &:= \frac{2 \left( \left( 1 - \frac{1}{1+N\kappa_{\min}} \right)^{-1/2} - 1 \right)}{\sqrt{\varepsilon/N}}, \quad n_{\text{sq}} := \frac{B_y + B_\alpha}{\sqrt{\varepsilon/N}}, \\ \tilde{n}_{\text{sq}} &:= \frac{B_w + B_\alpha}{\sqrt{\varepsilon/N^2}}, \quad n_{\text{inv}} := 3\sqrt{(N+1)/\varepsilon}, \quad \hat{n}_{\text{sq}} := \frac{B_w + 3}{\sqrt{\varepsilon/N}}, \end{aligned}$$

with  $B_w$  and  $B_\alpha$  defined in (15) and (20), respectively.

*Proof.* Let TF denote the complete transformer network constructed by composing the read-in blocks from Appendix C.2,  $\ell$  repetitions of the iteration blocks from Appendix C.3, and the read-out blocks from Appendix C.4. We set  $\epsilon_{\text{sq}}, \tilde{\epsilon}_{\text{sq}}, \hat{\epsilon}_{\text{sq}}, \epsilon_{\text{inv}}$  and  $\epsilon_{\text{flip}}$  in Proposition 11 to be  $\varepsilon$ , which gives

$$\begin{aligned} & \left| \text{readout}(\text{TF}(\mathbf{Z})) - \sum_{i=1}^N w_i^* \mathcal{K}(\mathbf{x}_i, \mathbf{x}_{N+1}) \right| \\ & \leq (1 - \eta\lambda_0(1-c))^\ell \frac{\left( \frac{1}{\sqrt{\lambda_0}} + 1 \right) B_y}{\lambda_0 \sqrt{\kappa_{\min}}} + \left( \frac{\frac{B_y}{\sqrt{\lambda_0}} + 2(1+\lambda_0)}{\lambda_0(1-c)\sqrt{\kappa_{\min}}} + \frac{1}{2} + \tilde{B}_w \right) \varepsilon. \end{aligned}$$

Moreover, we set  $\ell = L$  for  $L$  defined in (36), and it follows that  $(1 - \eta\lambda_0(1-c))^\ell \leq \varepsilon$ . Therefore,

$$\left| \text{readout}(\text{TF}(\mathbf{Z})) - \sum_{i=1}^N w_i^* \mathcal{K}(\mathbf{x}_i, \mathbf{x}_{N+1}) \right| \leq \left( \frac{\left( \frac{1}{\sqrt{\lambda_0}} + 1 \right) B_y}{\lambda_0 \sqrt{\kappa_{\min}}} + \frac{\frac{B_y}{\sqrt{\lambda_0}} + 2(1+\lambda_0)}{\lambda_0(1-c)\sqrt{\kappa_{\min}}} + \frac{1}{2} + \tilde{B}_w \right) \varepsilon.$$

The overall MLP width  $W$  is determined by taking the maximum of the widths required for the zero-out layers and each of the individual approximations (17), (21), (25), (28), and (30). This completes the proof.  $\square$

## D Classical solvers

In this section we review the four classical KRR solvers with their standard convergence rates in terms of the condition number  $\kappa$  of the system matrix. For all four methods, we initialize  $\mathbf{w}^{(0)} = \mathbf{0}$ .

**Preconditioned Richardson.** Preconditioned Richardson numerically solves the kernel system (2) with the update rule given in (3). We set  $\eta = 1/\text{eig}_{\max}(\mathbf{D}^{-1}(\mathbf{K} + \lambda\mathbf{I}))$ , and it requires  $\mathcal{O}(\kappa_{\mathbf{D}} \log(1/\varepsilon))$  steps to achieve  $\varepsilon$  error, where  $\kappa_{\mathbf{D}} := \kappa(\mathbf{D}^{-1/2}(\mathbf{K} + \lambda\mathbf{I})\mathbf{D}^{-1/2})$  and  $\kappa(\cdot)$  refers to the condition number of the matrix [Ryaben'kii and Tsynkov, 2006].

**Conjugate Gradient.** Conjugate Gradient is applied to the kernel system (2). With  $\mathbf{r}^{(0)} = \mathbf{y}$  and  $\mathbf{p}^{(0)} = \mathbf{r}^{(0)}$ , the update rule is  $\mathbf{w}^{(k+1)} = \mathbf{w}^{(k)} + \eta_k \mathbf{p}^{(k)}$ , where  $\eta_k = \frac{\|\mathbf{r}^{(k)}\|^2}{(\mathbf{p}^{(k)})^\top (\mathbf{K} + \lambda\mathbf{I}) \mathbf{p}^{(k)}}$ ,  $\mathbf{p}^{(k+1)} = \mathbf{r}^{(k+1)} + \frac{\|\mathbf{r}^{(k+1)}\|^2}{\|\mathbf{r}^{(k)}\|^2} \mathbf{p}^{(k)}$ , and  $\mathbf{r}^{(k+1)} = \mathbf{r}^{(k)} - \eta_k (\mathbf{K} + \lambda\mathbf{I}) \mathbf{p}^{(k)}$ . It requires  $\mathcal{O}(\sqrt{\kappa} \log(1/\varepsilon))$  steps to achieve  $\varepsilon$  error with  $\kappa = \kappa(\mathbf{K} + \lambda\mathbf{I})$  [Shewchuk, 1994].

**Gradient Descent.** Standard Gradient Descent (GD) is applied to the RKHS loss  $L(\mathbf{w}) = \frac{1}{2} \|\mathbf{K}\mathbf{w} - \mathbf{y}\|^2 + \frac{1}{2} \lambda \mathbf{w}^\top \mathbf{K}\mathbf{w}$ , with update rule  $\mathbf{w}^{(k+1)} = \mathbf{w}^{(k)} - \eta \mathbf{K}((\mathbf{K} + \lambda\mathbf{I})\mathbf{w}^{(k)} - \mathbf{y})$ . We select  $\eta = 1/\text{eig}_{\max}(\mathbf{K}(\mathbf{K} + \lambda\mathbf{I}))$  for GD, and it requires approximately  $\mathcal{O}(\kappa^2 \log(1/\varepsilon))$  steps to achieve  $\varepsilon$  error [Bach, 2024].

**Nesterov Gradient Descent.** On the same RKHS loss  $L(\mathbf{w})$ , Nesterov Gradient Descent has update rule  $\mathbf{w}^{(k+1)} = \mathbf{z}^{(k+1)} + \beta(\mathbf{z}^{(k+1)} - \mathbf{z}^{(k)})$ , where  $\mathbf{z}^{(k+1)} = \mathbf{w}^{(k)} - \eta \mathbf{K}((\mathbf{K} + \lambda \mathbf{I})\mathbf{w}^{(k)} - \mathbf{y})$ . Let  $\mathbf{A} := \mathbf{K}(\mathbf{K} + \lambda \mathbf{I})$ . Initializing  $\mathbf{z}^{(0)} = \mathbf{0}$ , we set  $\eta = 1/\text{eig}_{\max}(\mathbf{A})$  and  $\beta = (\sqrt{\text{eig}_{\max}(\mathbf{A})/\text{eig}_{\min}(\mathbf{A})} - 1)/(\sqrt{\text{eig}_{\max}(\mathbf{A})/\text{eig}_{\min}(\mathbf{A})} + 1)$ . It requires approximately  $\mathcal{O}(\kappa \log(1/\varepsilon))$  steps to achieve  $\varepsilon$  error [Bach, 2024].

## E Training and implementation details

This appendix gives the architectural, optimization, curriculum, probing, and evaluation details used for all experiments in Section 5. Unless otherwise stated, all reported results use the same training protocol, random seeds, and evaluation budget described below.

**Transformer architecture.** The detailed structure of the GPT-2-style transformer is listed in Table 1.

**Optimization.** All models are trained using hyperparameters listed in Table 2.

**Context-length curriculum.** Following the curriculum strategy used in [Bai et al., 2023, Fu et al., 2024], we train with a gradually increasing context length. This stabilizes optimization at the maximum context length  $N = 40$ . At training step  $s$ , the active context length is

$$n(s) = \min\{n_{\text{start}} + \lfloor s/\Delta s \rfloor \Delta n, N\},$$

with  $n_{\text{start}} = 11$ ,  $\Delta n = 2$ , and  $\Delta s = 2000$ . The curriculum reaches the maximum context length  $N = 40$  after approximately  $3 \times 10^4$  steps, after which all remaining training is performed at full context length.

Table 1: Default transformer architecture used in the main experiments.

Hyperparameter	Value
Layers $L$	12 (main experiments); 24 (depth ablation)
Heads $H$	8
Hidden width $d_{\text{model}}$	256
Feedforward width $d_{\text{ff}}$	1024 ( $= 4d_{\text{model}}$ )
Dropout	0.0
Layer normalization	Pre-LN
Activation	GELU
Positional encoding	Learned absolute embeddings
Attention mask	Causal

**Probe training.** After training the transformer, we freeze its weights and train a separate linear probe with weight  $\mathbf{W}_{\ell}^{\text{probe}} \in \mathbb{R}^{d_{\text{model}} \times 1}$  and bias  $b_{\ell}^{\text{probe}} \in \mathbb{R}$  for each layer  $\ell \in [L]$ . Each probe maps the hidden state at the final query  $x$ -token to a scalar prediction. Probes are trained for 500,000 steps on the same data distribution and context-length curriculum as the base model, using learning rate  $10^{-4}$ .

**Evaluation protocol.** SimE and per-layer MSE metrics are evaluated on 256 held-out test sequences with a fixed random seed; the same 256 sequences are shared across the transformer and all classical baselines so per-sequence comparisons are deterministic. Unless otherwise stated, the iterative baselines are run for 500 iterations, except for the  $\kappa \approx 10,000$  depth ablation, where we use 1,500 iterations. CG is run until convergence or for at most 100 iterations. For the arccosine-1 kernel experiment, we use the same evaluation budget as in the corresponding Gaussian kernel setting.

Table 2: Optimization hyperparameters for transformer training runs.

Hyperparameter	Value
Optimizer	AdamW
$\beta_1, \beta_2$	0.9, 0.999
Weight decay	$10^{-4}$
Initial learning rate	$10^{-4}$
Final learning rate	$10^{-5}$
Schedule	Cosine annealing
Training steps	500,000
Batch size	64
Gradient clipping	1.0
Loss	MSE on causal $x$ -token predictions

**Computational resources.** For all experiments, the transformer is trained on a single NVIDIA V100 or RTX A4000 GPU. Layer-wise probes are trained in parallel across 4 RTX A4000 GPUs. Depending on exact model size, hardware, and experimental setup, a full training run takes between 6 and 12 wall-clock hours. Memory requirements are relatively lax; RTX A4000s offered 16 GB VRAM while models generally required around 2 GB VRAM for training, with exceptions for size ablation studies.

## F Additional experimental results

### F.1 Convergence and similarity for 12-layer transformers

In Figure 3 we report the argmax trajectory  $t^*(\ell)$  for the uniform and Gaussian distributions, which each show the linear growth of the preconditioned Richardson method. In Figure 4 we show the corresponding error curves for the uniform and Gaussian distributions. We additionally plot heatmaps for all combinations of distribution and iterative method in Figure 5.

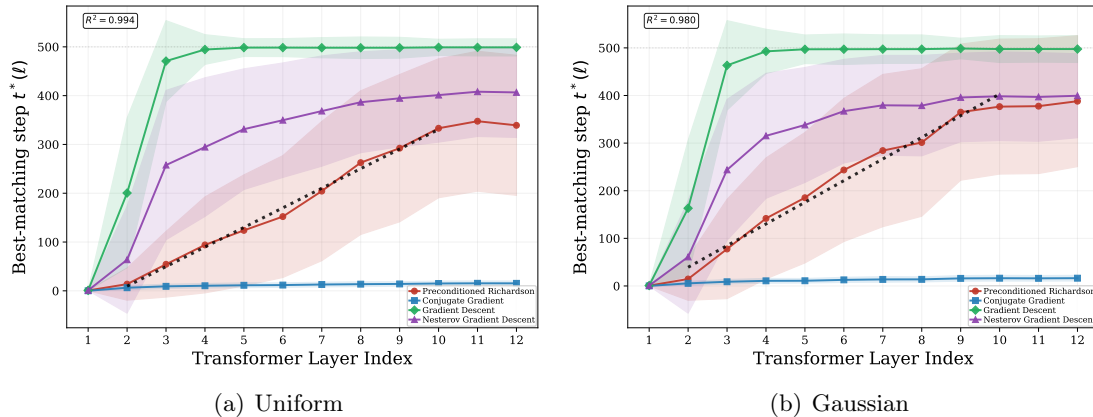


Figure 3: Best-matching step per transformer layer for Uniform and Gaussian inputs, supplementing the argmax plot of the spherical distribution in Figure 2. Preconditioned Richardson (red) exhibits a reliably linear growth across inner transformer layers. CG shows a higher characteristic speed that surpasses the transformer’s learned algorithm, while other methods are noticeably slower than the transformer and saturate earlier.

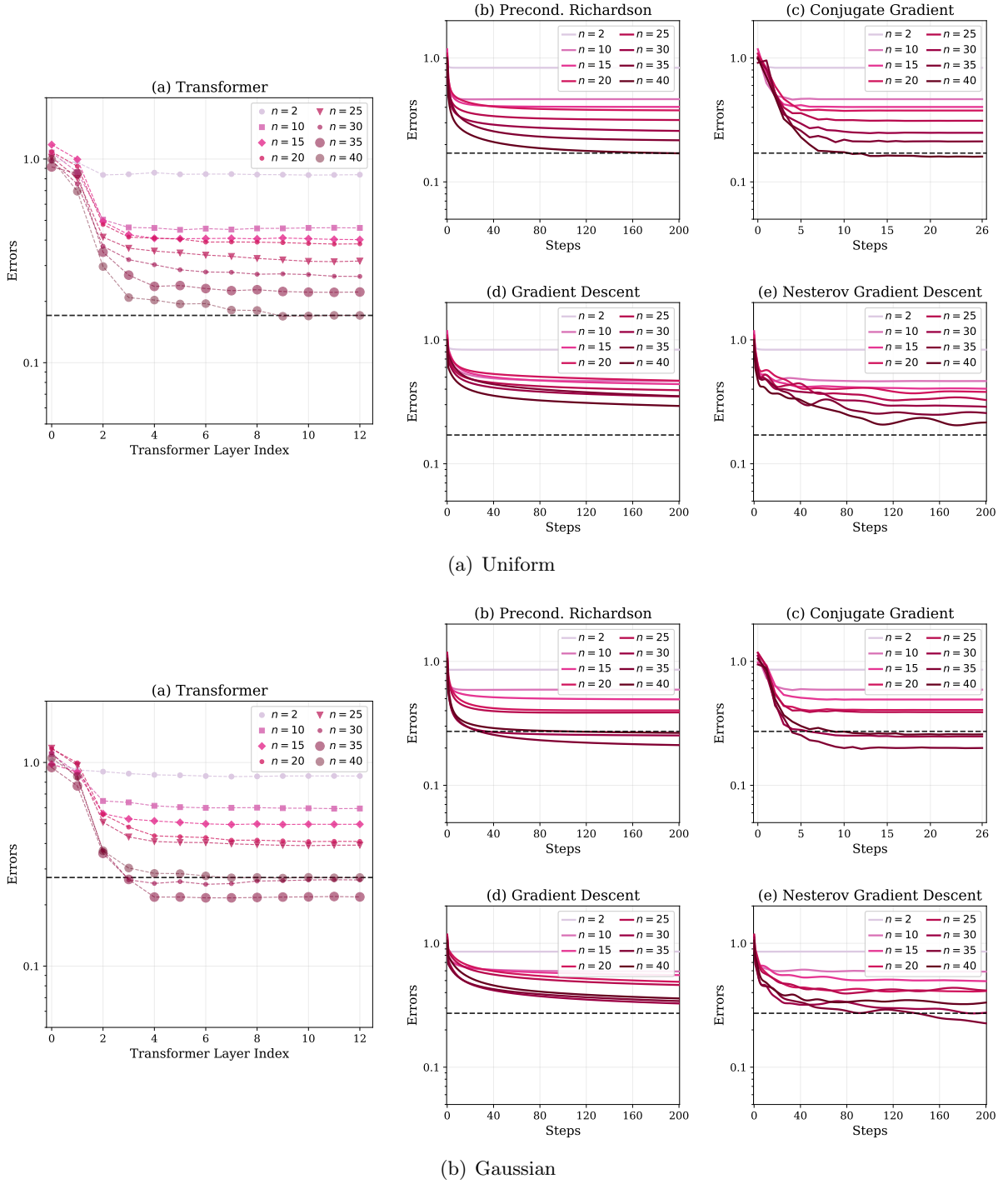


Figure 4: MSE convergence for (a) Uniform and (b) Gaussian input distributions, supplementing the spherical distribution in Figure 1 in the main text. All four classical methods are presented for comparison in each scenario.

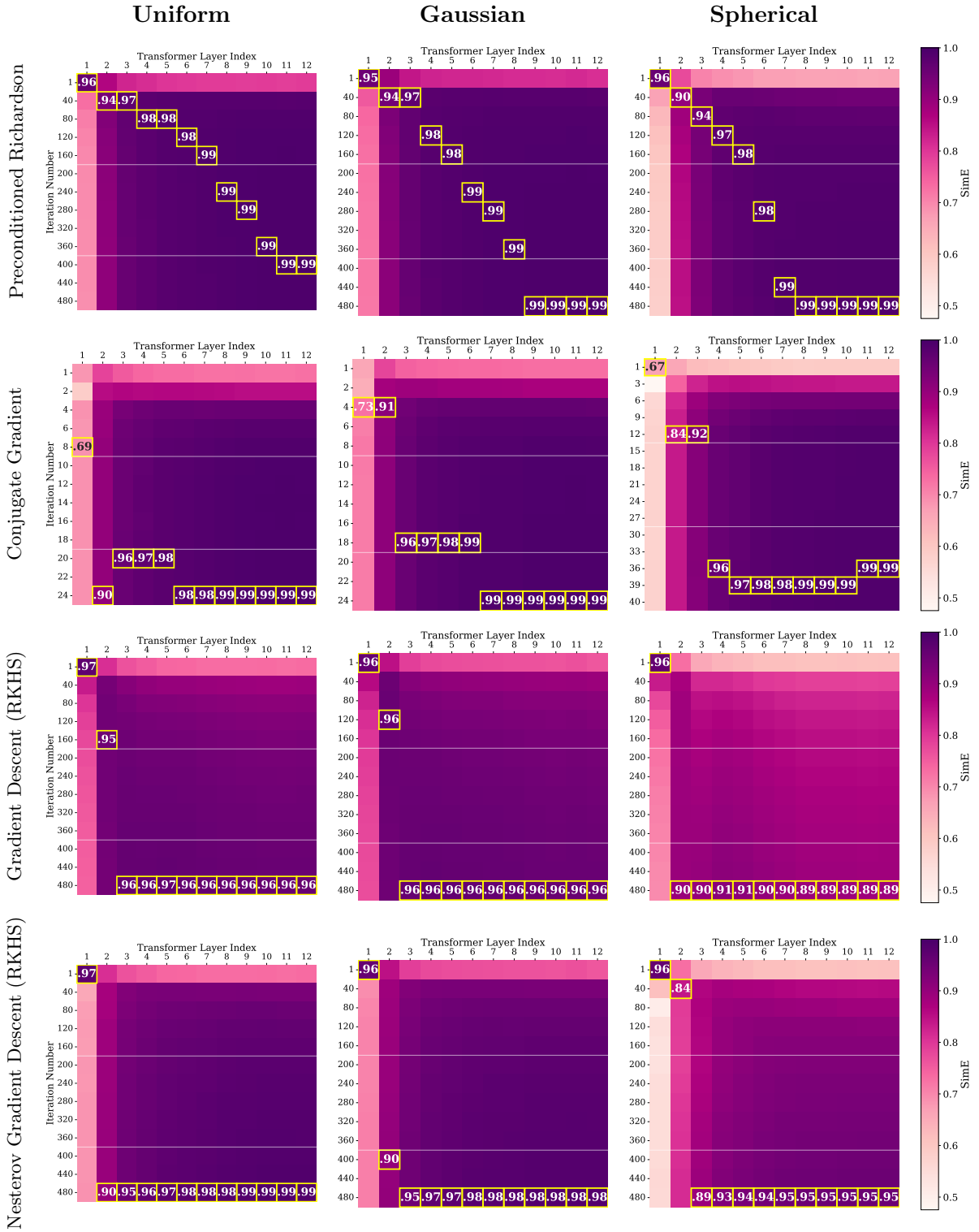


Figure 5: SimE heatmaps compare cosine similarity between transformer per-layer error vectors and classical solver per-iteration error vectors across four algorithms (rows) and three input distributions (columns), supplementing Figure 2. Yellow rectangles indicate the iteration with maximum SimE for each transformer layer, with annotations showing the corresponding SimE value. The color scale is shared across all panels.

## F.2 Depth ablation: 24-layer transformers

For depth ablation, we analyze spherical GP data with two different bandwidths  $v = 1$  and  $v = 2$ . In Figure 6 we plot error curves for both distributions with heatmaps in Figure 7.

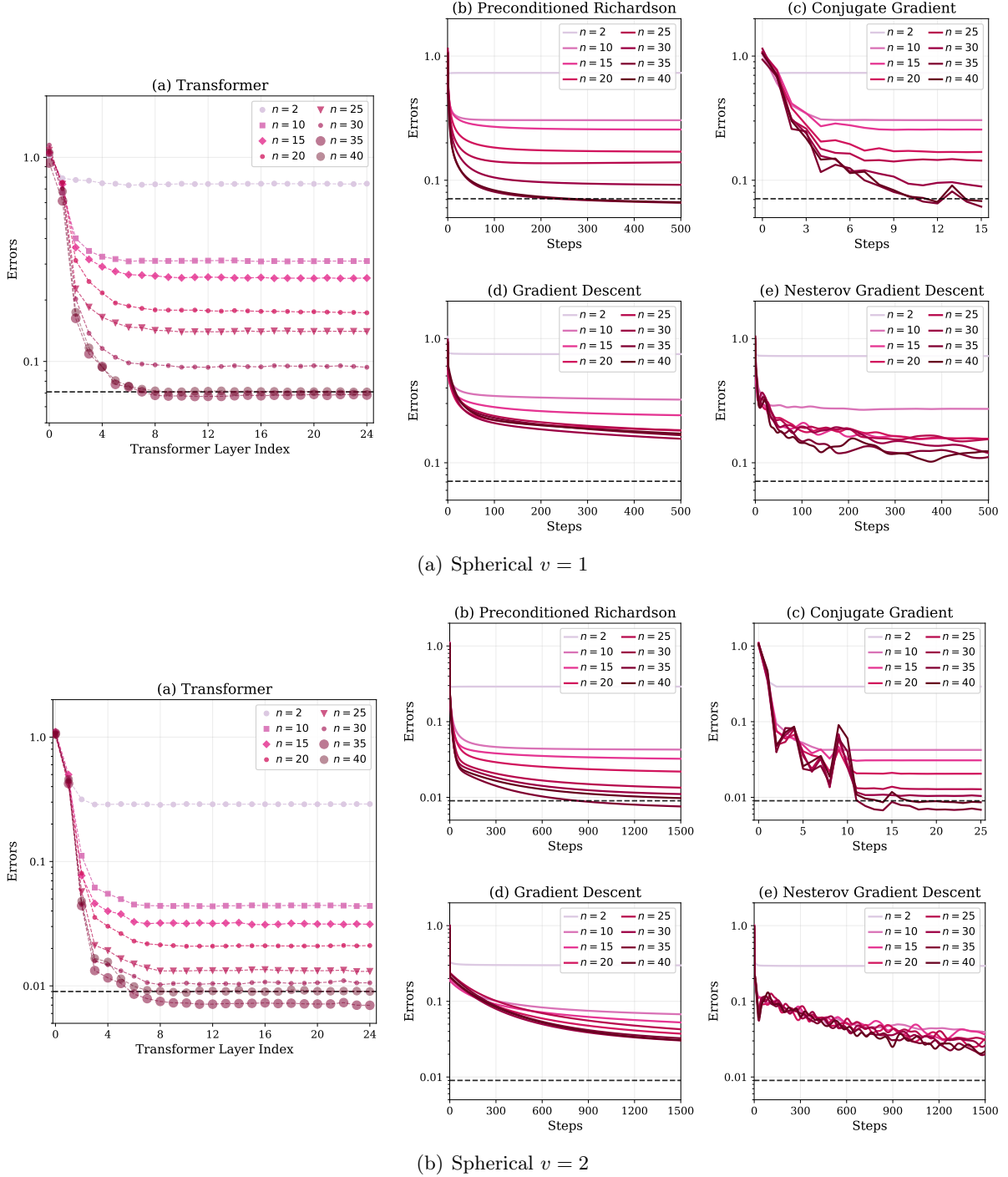


Figure 6: MSE convergence plots for the spherical distribution for 24 layer transformers, (a) using  $v = 1$  or (b) using  $v = 2$ . Even at increased depth, a strong match with preconditioned Richardson iterations is evident, and both forms of gradient descent still fail to reach the transformer’s level of accuracy in the allotted iterations.

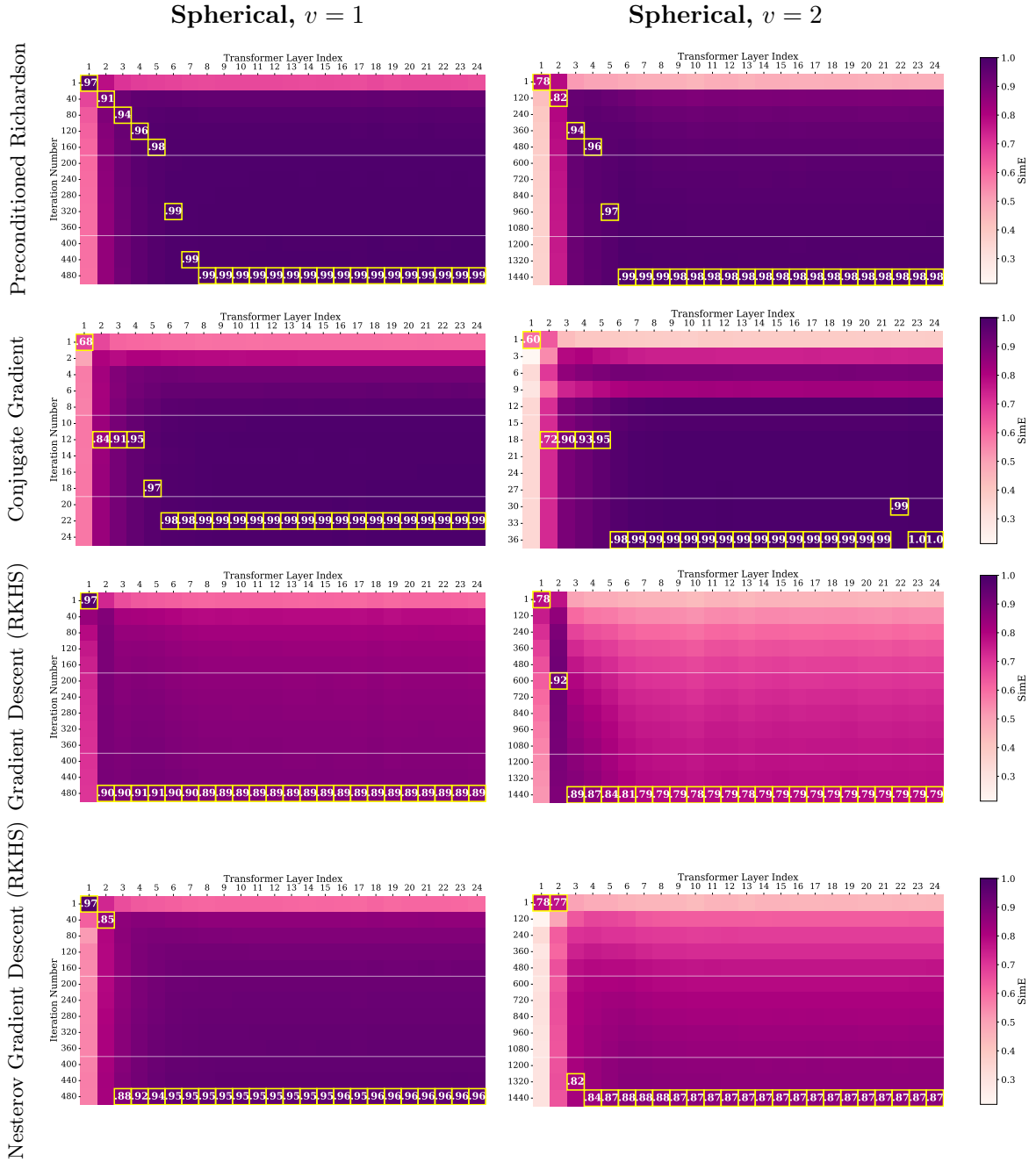


Figure 7: SimE heatmaps for the 24-layer depth ablation using the spherical distribution and Gaussian kernel. Left column: bandwidth  $v = 1$  with  $\kappa \approx 3,000$  and 500-step iteration budget. Right column: bandwidth  $v = 2$  with  $\kappa \approx 10,000$  and 1500-step iteration budget. Rows from top: Preconditioned Richardson, Conjugate Gradient, Gradient Descent (RKHS loss), Nesterov Gradient Descent (RKHS loss). Yellow boxes mark the iterative step with highest SimE per transformer layer. Color scale is shared across all panels. In conjunction with Figure 6 we see evidence of a linear trend for preconditioned Richardson, though more clearly localized to earlier layers than in the 12-layer experiment heatmaps shown in Figure 5.

### F.3 Convergence curves for linear attention

We train transformers with linear attention rather than softmax attention with an otherwise identical experimental setup to Section 5.1. In Figure 8, we no longer see strong correspondence between error curves for the transformer and iterative methods, and the argmax plots do not show a single method performing with high linearity across all three distributions.

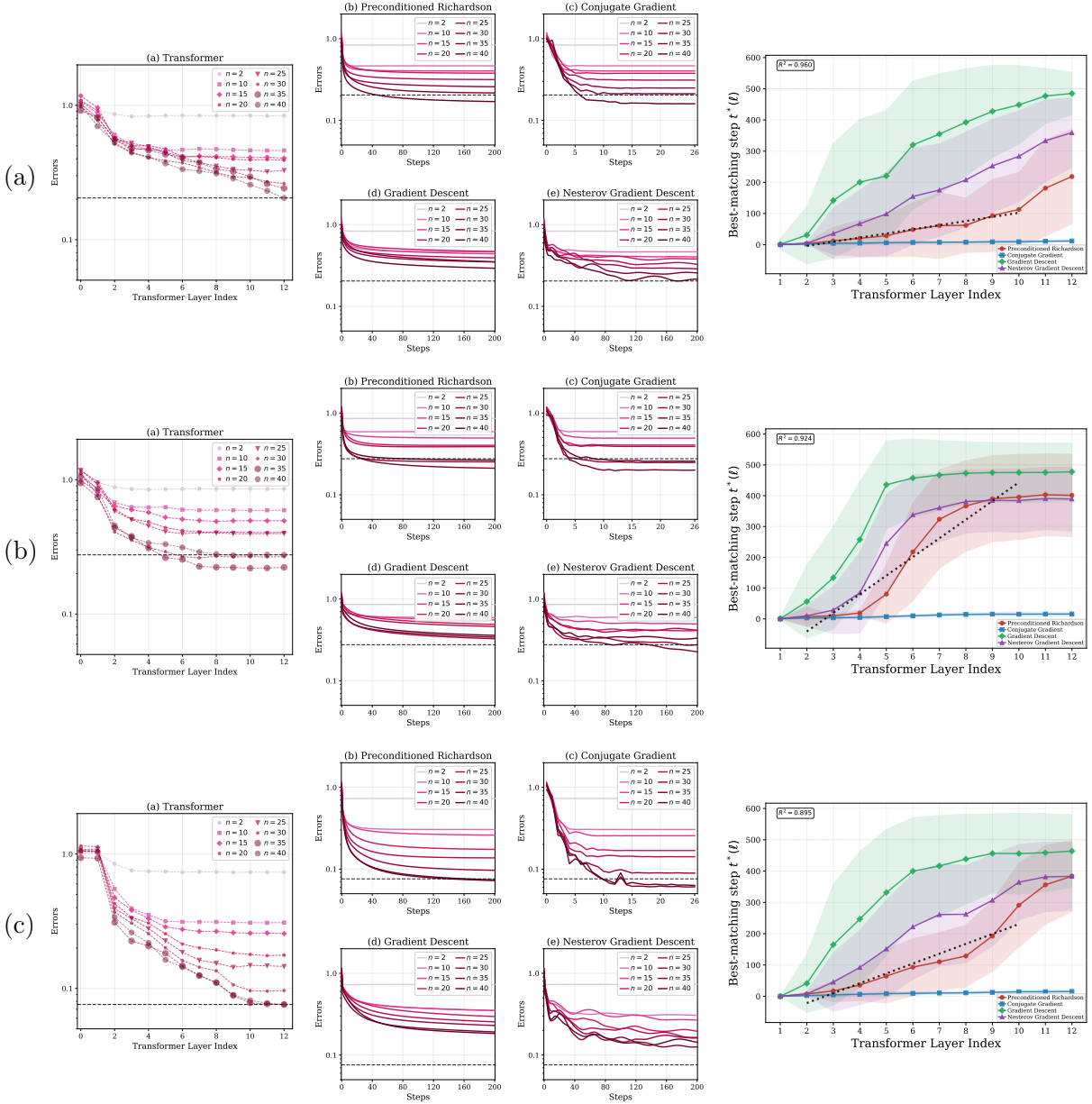


Figure 8: MSE convergence and argmax step maps for linear attention under (a) Uniform, (b) Gaussian, and (c) Spherical distributions. While some argmax plots show linearity, no single method is capable of high linearity across all distributions as seen with softmax attention in Figures 2 and 3.

## F.4 Architecture ablations: width and number of heads

In Figure 9 we plot the effect of additional attention heads and MLP width on the trained transformer error. Increasing head count has minimal impact, consistent with Theorem 1 where a single head can realize the relevant iterative computation. In contrast, increasing the model width results in prediction error decreasing rapidly and then remaining near the KRR baseline past an initial width threshold.

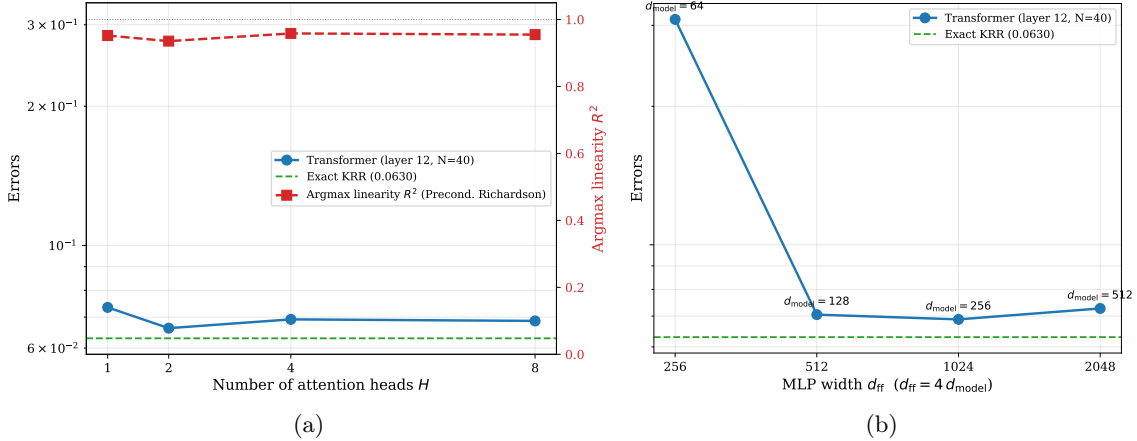


Figure 9: Heads and widths ablation studies on 12-layer transformers trained on spherical GP data. (a) Effect of varying the number of attention heads  $H \in \{1, 2, 4, 8\}$  while holding total parameter count fixed via  $d_{\text{head}} = d_{\text{model}}/H$ . The linearity observed in the argmax plot is also shown in orange and remains close to 1. (b) Final-layer prediction error at  $N=40$  with respect to model width, with  $d_{\text{ff}} = 4d_{\text{model}}$ . Both are compared against the exact KRR baseline in green.

## F.5 Noise-mismatch ablation: behavioral evidence for finite-depth Richardson with fixed $\lambda$

The construction in Appendix C fixes the regularization parameter  $\lambda$  at construction time and runs  $L$  Richardson steps. If a trained transformer realizes the same mechanism, two predictions follow. (i) *The effective  $\lambda$  is fixed.* The transformer should regularize at a single  $\lambda$  regardless of  $\sigma_{\text{test}}$ , rather than adapting per query as a Bayes-optimal predictor would. (ii) *Finite depth biases the iterate toward zero.* An  $L$ -step Richardson iterate is partway between  $\mathbf{w} = \mathbf{0}$  and the converged KRR solution at  $\lambda$ . Compared to converged KRR with the same  $\lambda$ , this truncation amplifies the predictor’s bias when that converged solution is already over-regularized (i.e., at  $\sigma_{\text{test}} \ll \sigma_{\text{train}}$ ), and acts as implicit early stopping which reduces variance when that converged solution would overfit (i.e., at  $\sigma_{\text{test}} \gg \sigma_{\text{train}}$ ).

We test both predictions by training a 12-layer transformer at a single training noise  $\sigma_{\text{train}} = 0.05$  and evaluating on test sequences with  $\sigma_{\text{test}} \in \{10^{-3}, 510^{-3}, 10^{-2}, 210^{-2}, 0.05, 0.1, 0.2, 0.5, 1.0\}$ . We compare the transformer’s final-layer MSE against two converged-KRR references evaluated on the same test sequences: *Bayes-optimal* ( $\lambda = \sigma_{\text{test}}^2$ , optimal for the actual test noise) and *encoded* ( $\lambda = \sigma_{\text{train}}^2$ , optimal for the training noise regardless of the test noise). All MSEs are computed against the noiseless ground-truth function  $f(\mathbf{x}_q)$ , so that the Bayes-optimal predictor is the minimizer of  $\mathbb{E}[(\hat{f}(\mathbf{x}_q) - f(\mathbf{x}_q))^2 | \text{data}]$ .

Figure 10 corroborates both predictions, with the same finite- $L$  truncation producing the asymmetry across regimes. *Prediction (i)*: across all three input distributions, both the transformer and the encoded oracle remain above Bayes-optimal at every  $\sigma_{\text{test}} \neq \sigma_{\text{train}}$ ; neither adapts

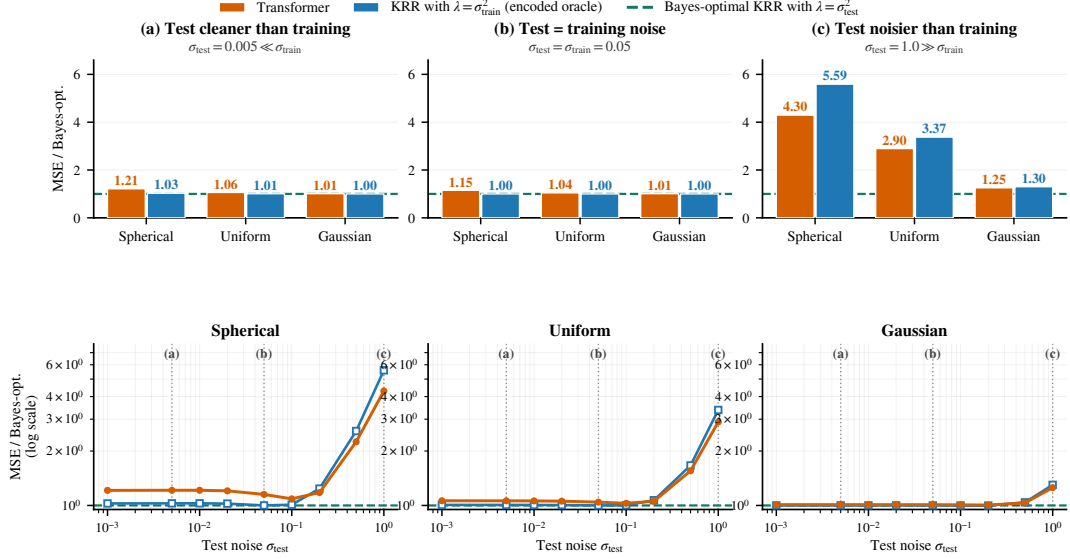


Figure 10: **Noise-mismatch ablation: three regime snapshots and the full sweep.** All MSEs are reported relative to Bayes-optimal converged KRR (dashed line at 1.0); values above 1.0 are over-regularized relative to Bayes-optimal. *Top row (regime snapshots):* (a)  $\sigma_{\text{test}} \ll \sigma_{\text{train}}$ : both transformer (orange) and encoded oracle (blue) sit above Bayes-optimal, as neither adapts  $\lambda$  down for cleaner test data, and the transformer is above the encoded oracle (e.g., 1.21 vs. 1.03 on Spherical), because finite- $L$  truncation amplifies the over-regularization. (b)  $\sigma_{\text{test}} = \sigma_{\text{train}}$ : the encoded oracle coincides with Bayes-optimal, and the transformer is within 1–15% of both, with the residual gap attributable to the  $L = 12$  truncation. (c)  $\sigma_{\text{test}} \gg \sigma_{\text{train}}$ : the transformer sits below the encoded oracle in every distribution, with transformer-to-encoded ratios 0.77/0.86/0.97 on Spherical/Uniform/Gaussian, because the same finite- $L$  truncation acts as early stopping and prevents the converged  $\lambda = \sigma_{\text{train}}^2$  solution from overfitting the larger test noise. *Bottom row (continuous sweep over  $\sigma_{\text{test}}$ ):* the same two predictors plotted across all nine test-noise levels, one panel per input distribution. Vertical dotted lines mark the snapshot positions (a)/(b)/(c). Transformer and encoded curves cross near  $\sigma_{\text{test}} = \sigma_{\text{train}}$ , separating into the two regimes shown above; the smooth transition is a single signature of finite-depth Richardson with a fixed  $\lambda$ , not two separate effects. Numerical values at every sweep point are reported in Table 3.

$\lambda$  to  $\sigma_{\text{test}}$ . *Prediction (ii):* at  $\sigma_{\text{test}} \ll \sigma_{\text{train}}$ , the transformer sits above the encoded oracle (the truncation pushes a partly-converged iterate further toward  $\mathbf{0}$  than the already over-regularized converged KRR); at  $\sigma_{\text{test}} \gg \sigma_{\text{train}}$ , the transformer sits below the encoded oracle (the truncation prevents the converged solution from fitting the larger noise). The bottom row of Figure 10 shows the two transitions as a single continuous crossover at  $\sigma_{\text{test}} \approx \sigma_{\text{train}}$ , and Table 3 reports the exact values at every sweep point. The whole sweep is thus consistent with the single mechanism of finite-depth Richardson with  $\lambda \approx \sigma_{\text{train}}^2$  rather than two separate effects. This presents a behavioral equivalence: the data shows the transformer behaves as if it were running finite-depth Richardson with  $\lambda \approx \sigma_{\text{train}}^2$ .

Table 3: **Noise-mismatch ablation, full sweep.** MSE relative to Bayes-optimal converged KRR for the trained transformer (TF), the encoded oracle (EO, i.e., converged KRR with  $\lambda = \sigma_{\text{train}}^2$ ), and the Bayes-optimal (BO, i.e., converged KRR with  $\lambda = \sigma_{\text{test}}^2$ ), across the nine test-noise levels and three input distributions. By construction, BO = 1.00 everywhere; values above 1.00 are over-regularized. The row marked † corresponds to  $\sigma_{\text{test}} = \sigma_{\text{train}}$ , where EO and BO coincide. The transformer sits above EO for  $\sigma_{\text{test}} \leq 0.1$  (truncation amplifies over-regularization on already-over-regularized converged KRR) and below EO for  $\sigma_{\text{test}} \geq 0.2$  (truncation prevents converged KRR from overfitting the larger noise), with the crossover near  $\sigma_{\text{test}} \approx \sigma_{\text{train}}$ . Ratios reported in Figure 10 are computed from unrounded MSEs; the two-decimal entries below are rounded for readability.

$\sigma_{\text{test}}$	Spherical			Uniform			Gaussian		
	TF	EO	BO	TF	EO	BO	TF	EO	BO
$10^{-3}$	1.21	1.03	1.00	1.06	1.01	1.00	1.01	1.00	1.00
$5 \cdot 10^{-3}$	1.21	1.03	1.00	1.06	1.01	1.00	1.01	1.00	1.00
$10^{-2}$	1.21	1.03	1.00	1.06	1.01	1.00	1.01	1.00	1.00
$2 \cdot 10^{-2}$	1.20	1.02	1.00	1.06	1.00	1.00	1.01	1.00	1.00
† $5 \cdot 10^{-2}$	1.15	1.00	1.00	1.04	1.00	1.00	1.01	1.00	1.00
0.1	1.09	1.01	1.00	1.03	1.00	1.00	1.01	1.00	1.00
0.2	1.18	1.24	1.00	1.05	1.07	1.00	1.01	1.00	1.00
0.5	2.25	2.58	1.00	1.55	1.66	1.00	1.03	1.04	1.00
1.0	4.30	5.59	1.00	2.90	3.37	1.00	1.25	1.30	1.00